

Facial-Sketch Synthesis: A New Challenge

Deng-Ping Fan¹, Ziling Huang^{†2}, Peng Zheng^{†3}, Hong Liu^{*4}, Xuebin Qin^{*3} and Luc Van Gool¹

¹Computer Vision Lab, ETH Zürich, Zürich, Switzerland.

²Information and Communication Engineering, University of Tokyo, Tokyo, Japan.

³Computer Vision, MBZUAI, Abu Dhabi, UAE.

⁴Digital Content and Media Sciences Research Division, NII, Tokyo, Japan.

Abstract

This paper aims to conduct a comprehensive study on facial-sketch synthesis (FSS). However, due to the high costs of obtaining hand-drawn sketch datasets, there lacks a complete benchmark for assessing the development of FSS algorithms over the last decade. We first introduce a high-quality dataset for FSS, named **FS2K**, which consists of 2,104 image-sketch pairs spanning three types of sketch styles, image backgrounds, lighting conditions, skin colors, and facial attributes. FS2K differs from previous FSS datasets in difficulty, diversity, and scalability and should thus facilitate the progress of FSS research. Second, we present the largest-scale FSS investigation by reviewing **89** classical methods, including **25** handcrafted feature-based facial-sketch synthesis approaches, **29** general translation methods, and **35** image-to-sketch approaches. Besides, we elaborate comprehensive experiments on the existing **19** cutting-edge models. Third, we present a simple baseline for FSS, named **FSGAN**. With only two straightforward components, *i.e.*, facial-aware masking and style-vector expansion, FSGAN surpasses the performance of all previous state-of-the-art models on the proposed FS2K dataset by a large margin. Finally, we conclude with lessons learned over the past years and point out several unsolved challenges. Our code is available at <https://github.com/DengPingFan/FSGAN>.

Keywords: Facial sketch synthesis, facial sketch dataset, benchmark, attribute, style transfer

1 Introduction

Facial-sketch synthesis (FSS) aims to generate gray-scale sketches from RGB images of human faces (image-to-sketch, I2S) or the other way around (sketch-to-image, S2I) [1, 2]. FSS is commonly used by law enforcement or used in surveillance to assist in face recognition and retrieval, based on a sketch drawing from an eyewitness [1]. For entertainment, it is also used in mobile apps, such as TikTok and Facebook.

Besides, it is an attractive topic in digital entertainment [3]. Research into FSS has achieved significant progress over the past decade.

Different from other face-related datasets, such as those for face recognition [13–15], face detection [16], face key-points detection [17], face alignment [18], and face synthesis [19], which can be manually labeled by annotators with limited training, face sketch datasets are much more difficult to obtain because only professional artists can produce high-quality references. Due to the high costs of obtaining professional sketches, existing image-sketch datasets [1, 2, 10] are relatively small with

[†] Contributed equally. ^{*} Corresponding authors.

Table 1 Comparison with other FSS datasets.

Dataset	Year	Pub.	Total	Train	Test	Att.	Public	Paired	Resolution
CUFS [1]	2009	TPAMI	606	306	300	×	✓	✓	200 × 250
IIIT-D [4]	2010	BTAS	231	58	173	×	×	✓	-
CUFSF [5]	2011	CVPR	1,194	500	694	×	✓	✓	779.62±15.05 × 812.10±13.92
VIPSL [6, 7]	2011	TCSVT	1,000	100	900	×	×	✓	-
DisneyPortrait [8]	2013	TOG	672	-	-	×	×	✓	-
UPDG [9]	2020	CVPR	952	798	154	×	×	×	-
APDrawing [10]	2020	TPAMI	140	70	70	×	✓	✓	512 × 512
FS2K (Ours)	2022	MIR	2,104	1,058	1,046	✓	✓	✓	299.74±95.07 × 273.56±38.67

* Att. = Attributes. In [11] and [12], CUFS is divided into 268 and 338 images for training and testing. For image resolution, we provide the width and height as $W_{avg} \pm W_{std}$ and $H_{avg} \pm G_{std}$, respectively. W_{avg} and W_{std} denote the mean value and standard deviation, respectively.

limited diversity. This dataset shortage has limited the development, especially for data-hungry deep learning models.

In addition, how to evaluate FSS remains an open question. Structural similarity (SSIM) [20] is one of the most widely used metrics for evaluating image quality, so also it is typically used to assess the performance of S2I models. Nevertheless, the characteristics of facial sketches are very different from RGB-based facial images, which makes it challenging to apply the current evaluation metrics to I2S tasks. Therefore, a new objective and quantitative metric, which is also highly consistent with human assessment, is needed for benchmarking the FSS task.

Moreover, due to the lack of *high-quality datasets* and *proper evaluation metrics*, different FSS models (*e.g.*, [1, 2]) are usually built and tested upon diverse training datasets¹ and with different evaluation methods. Hence, it isn't easy to provide fair and comprehensive comparisons. Further, many cutting-edge transformation models (*e.g.*, CycleGAN [21], UNIT [22], Pix2pixHD [23], SPADE [24], DMAP [25], NICEGAN [26], and DRIT++ [27]) designed for related image-to-image transfer tasks could potentially be employed in FSS tasks. However, as mentioned above, these models lack performance evaluation for the FSS task because of the shortage of datasets and evaluation metrics. Therefore, thorough comparisons and assessments of FSS-related models on a standard FSS dataset with unified evaluation metrics are long overdue. To this end, we have introduced and maintained an online paper list (<https://github.com/DengPingFan/FaceSketch-Awesome-List>) to track the progress of this fast-developing field.

1.1 Contributions

Our goal is to solve the discussed issues (*i.e.*, limited datasets, metrics, and benchmarks) and further contribute to a new challenge for the FSS community. The main contributions are:

- 1) **FSS Dataset.** We build a new high-quality FSS dataset, termed **FS2K**. It is the largest (see Table 1) publicly released FSS dataset,² consisting of 2,104 image-sketch pairs with a wide range of image backgrounds, skin patches, sketch styles, and lighting conditions. In addition, we also provide extra attributes, *e.g.*, *gender*, *smile*, *hair style*, *etc.*, to enable deep learning models to learn more detailed cues.
- 2) **FSS Review and Benchmark.** We conduct the largest-scale FSS study, reviewing 89 representative approaches, including 25 methods using handcrafted features, 29 models for the general transfer task, and 35 I2S transfer algorithms. Based on our FS2K, we adopt the SCOOT metric [29] and conduct a rigorous evaluation of 19 state-of-the-art models from the perspective of content and style.
- 3) **FSS Baseline.** We design an efficient GAN-based baseline, termed **FSGAN**, which consists of two simple core components, *i.e.*, facial-aware masking and style-vector expansion. The former is utilized to restore details of the facial components, while the latter is adopted to learn different face styles. FSGAN serves as a unified baseline model for both I2S and S2I tasks (Fig. 1) on our newly built FS2K dataset. Our project is available at <https://github.com/DengPingFan/FSGAN>.

²Establishing an FSS dataset drawn by professional artists is more challenging than other face datasets, *e.g.*, face attribute datasets [28], which is why the largest existing FSS dataset, *i.e.*, CUFSF [5], has only ~1K images in the past 13 years. Although FS2K is only ~2 times larger than CUFSF, we still took one year to create such a high-quality dataset.

¹Because they want to learn a different style of sketches.

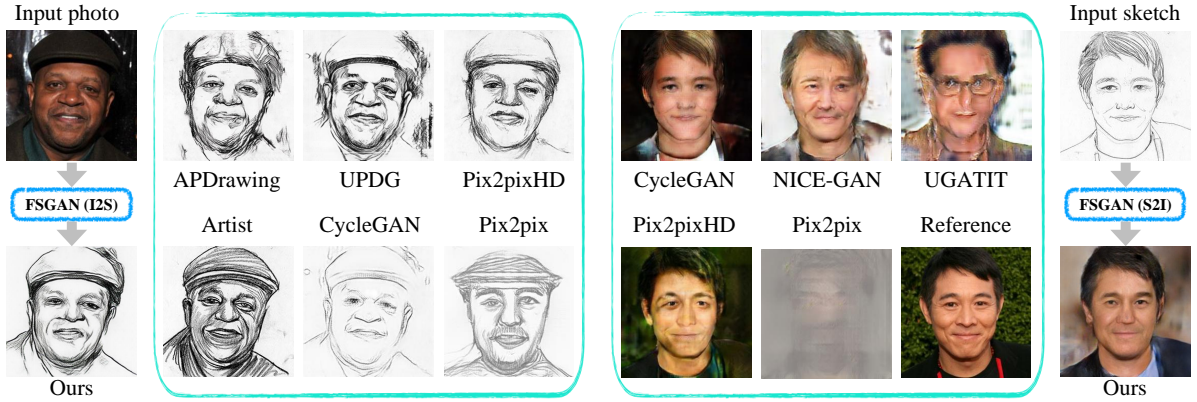


Fig. 1 **Left:** Our FSGAN (I2S) learns from artist drawings and intelligently turns an input photo into a vivid face sketch. In contrast, the five cutting-edge style transfer approaches cannot obtain visually appealing results. Only UPDG [9] and Pix2pixHD [23] perform relatively well, but they generate worse content and style than FSGAN. **Right:** Given a sketch, our FSGAN (S2I) can also transform the input into a vivid facial photo. Meanwhile, the results from the five representative deep learning models are either structurally damaged (*i.e.*, CycleGAN [21], NICE-GAN [26], and UGATIT [30]) or blurry (*i.e.*, Pix2pix [31]). More results can be found in Fig. 8-11.

- 4) **Discussions and Future Directions.** In addition to an overall performance assessment, we also conduct an attribute-level evaluation, present detailed discussions, and explore some promising future directions.

2 Related Works

This section first conducts a complete literature review of the existing FSS datasets. Then, in the second part, we discuss the taxonomy of facial synthesis and highlight particularly innovative and successful approaches for this task, including traditional facial synthesis, image-to-image translation, neural style transfer, and deep photo-sketch synthesis. The taxonomy of facial-sketch synthesis is shown in Fig. 3. A summary of the models, including their key innovations, datasets, code links, and citation information, can be found in Table 2 and Table 3.

2.1 Dataset

We outline four classical datasets for the FSS task, *i.e.*, CUFS [1], IIIT-D [4], CUFSF [5], VIPSL [7], and three portrait sketching datasets [8–10], which are the basis for building most FSS models [32].

CUFS [1] is one of the earliest and most commonly used datasets. It contains 606 photo-sketch pairs, which include 123 samples from the AR face database [33], 188 samples from the

CUHK student database, and 295 samples from the XM2VTS database [34]. A sketch drawn by an artist and a corresponding photo is provided for each sample. Each photo is taken in a frontal pose under normal lighting conditions and maintains a neutral expression. All three sub-databases use solid backgrounds, *e.g.*, cyan, white, blue, *etc.* However, real-world scenes are complex and diverse, and it is difficult to guarantee that photo will be captured in such a fixed environment. Besides, the sketches in this dataset were created by the same artist, so they are of limited style.

CUFSF [5] is a commonly used database for assessing the performance of FSS models. It contains 1,194 photo-sketch pairs, collected from the FERET database [35]. An artist drew all sketches after viewing the corresponding photo. CUFSF has a similar photo collection environment to CUFS but is more challenging. Because the photos in the dataset undergo illumination changes, each face has low contrast with the background, and each sketch contains exaggerated shapes.

VIPSL [7] contains 200 face photos collected from the FRAV2D [36], FERET [35], and Indian face databases [7]. Unlike CUFS and CUFSF, VIPSL has five sketches for each face, drawn by five artists with different styles, while viewing the same photo under the same conditions as CUFS.

IIIT-D [4, 37] consists of three types of sketch databases, including a viewed sketch database, a semi-forensic sketch database, and a forensic

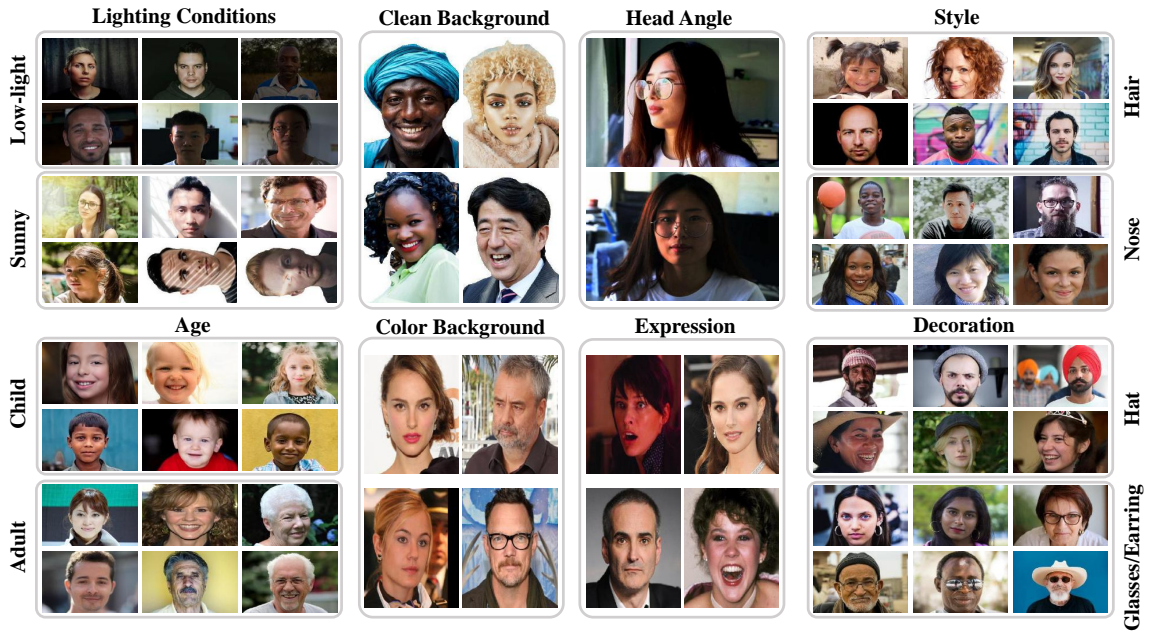


Fig. 2 Representative image samples from our FS2K. The collected images depict diverse scenes according to different selection criteria, such as various lighting conditions (*i.e.*, low-light, sunny), ages (*i.e.*, child or adult), backgrounds (*i.e.*, clean or colored), head angles, facial expressions (*e.g.*, serious, smiling, and laughing), hair styles (*e.g.*, black, blonde, long, and short), and accessories (*i.e.*, hat or earrings).

sketch database. All photos are derived from the CUHK student database and IIIT-Delhi Sketch database [4]. The first viewed sketch database contains 238 sketch-digital image pairs, with all sketches drawn by the professional artist based on a given photo. The second sub-database has 140 sketch-face image pairs, where all the sketches are drawn by memory after the artist has observed the corresponding photo. The third forensic sketch database consists of 190 sketches that a sketch artist draws according to the description of an eyewitness based on their recollection of a crime scene. IIIT-D contains multiple styles of sketch portraits, making it more challenging. However, obtaining forensic sketches is tricky since they are usually derived from law enforcement.

Portrait Sketching Dataset. Yi *et al.* [9, 10] provided two datasets that simulate artistic portrait drawing (APDrawing). The first dataset [10] contains 140 pairs of face photos and corresponding sketch portraits drawn by a single portrait artist. This was later extended to a larger dataset in [9], with 952 face photos and 625 portrait sketches. Of the collected photos, 220 of them are from three famous painters, and the remaining

212 photos are from a photography website.³ It is worth noting that the photos and portraits in this dataset are not paired. Disney Research published a portrait dataset [8] composed of 24 faces from the face database [38] and 672 sketches from seven artists under four levels of abstraction. Besides, they also provided each stroke as a transparent bitmap to be used later to create new sketches.

Unlike existing datasets, we provide a more challenging, high-quality, and attribute-annotated dataset, which is currently the largest dataset of facial-sketch synthesis. The new dataset contains 2,104 pairs of photos and sketches, 1,058 used for model training, and the remaining for evaluation. The strengths of our FS2K include multiple drawing styles, highly accurate alignment between sketches and photos, multiple attribute information, complex backgrounds, *etc.* Detailed comparisons of the datasets are shown in Table 1.

2.2 Traditional Facial Synthesis

Researchers used heuristic image transformations to interactively or automatically synthesize facial

³<https://vectorportal.com/>

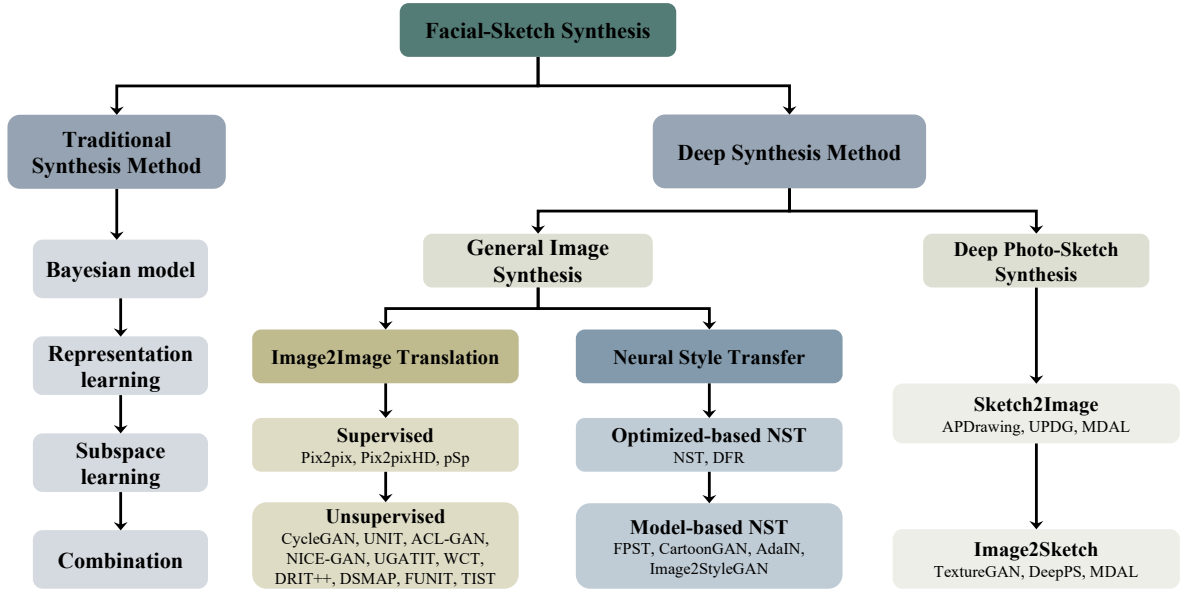


Fig. 3 A taxonomy of facial-sketch synthesis and the representative methods.

sketches [3, 39–43] in the early years. However, these methods tend to generate artificial and inexpressive sketches that lack artistic style. Therefore, in recent years, more attention has been focused on learning-based facial synthesis schemes, whose taxonomy is shown in Fig. 3. These can be categorized into Bayesian inference models, representation learning models, subspace learning models, *etc.*

2.2.1 Bayesian Inference Models

Bayesian inference exploits evidence to update the states of the sketch components over probability models, which has been widely used in FSS [44]. In [45], Chen *et al.* firstly introduced an example-based facial-sketch synthesis system that uses a non-parametric sampling algorithm to learn subtle sketch styles. Later, the embedded hidden Markov model [46] was used to model the non-linear relationships in photo-sketch pairs, followed by a selective ensemble strategy to generate facial sketches [47]. Wang and Tang [1] followed a similar idea but considered face structures across different scales, using a multi-scale Markov Random Field (MRF) to build the relationships between photo-sketch pairs. Xu *et al.* [48] proposed a hierarchical compositional model that considers faces' regularity and structural variation. These methods have made significant progress in generating

sketches, but they only consider simple controlled conditions, ignoring variations in lighting and pose. Zhang *et al.* [49] addressed this by simultaneously considering patch matching, intensity compatibility, gradient compatibility, and shape priors, resulting in better visual effects. However, MRF-based models have two main drawbacks: (1) They struggle to synthesize unseen facial information; (2) Their optimization is NP-hard. Zhou *et al.* [50] used Markov weight fields and cascaded decomposition to build a robust facial synthesis system, using a linear combination of candidate patches to approximate new sketch patches. Wang *et al.* [51] built a non-parametric model to transform a photograph into a portrait painting, where an MRF is used to enhance the spatial coherence of the style parameters, and an active shape model and a graph-cut model are used to learn the local information of facial features. Wang *et al.* [52] presented a transductive learning method to synthesize facial sketches, which employs an on-the-fly optimization process to minimize the loss of the given test samples. Peng *et al.* [53] designed a superpixel method built on the Markov model to improve the flexibility without dividing the photo into regular rectangular patches. Then, they not only used the Markov network to model the relationships between image patches but also retained many visual aspects of the cues (such as edges) through multiple visual features [54].

2.2.2 Subspace Learning Models

Subspace learning has been widely studied in the FSS task [44], which is to learn a low dimensional manifold space embedded in a high dimensional space [55]. Tang and Wang [56–58] proposed a series of example-based approaches based on the linear eigen-transformation method. These methods are global linear systems, and they cannot fully explain the relationships between photo-sketch pairs because such a transformation is not a simple linear relationship. Liu *et al.* [59] used the LLE to handle this problem, making photo and sketch patches have manifolds with similar local geometric shapes in two different image spaces. However, the pseudo-image generation and the representation learning are divided into two independent processes, leading to sub-optimal results. Huang and Wang [60] proposed a joint learning framework, which contains domain-specific dictionary learning and subspace learning.

2.2.3 Representation Learning Models

Sparse coding and dictionary learning, *a.k.a.* representation learning, are used for the FSS task [44]. Ji *et al.* [61] demonstrated that personalized features are not effectively captured through the synthesis process. As such, several works [61–63] use different regression models, such as k-NN [61], Lasso [61], multivariate output regression [62], and support vector regression [63], to build the transformation between photos and sketches. To improve the quality of the generated facial sketches, Wang *et al.* [6, 7] used the local linear embedding (LLE) [64] to estimate an initial sketch or photo and then introduced a sparse multi-dictionary representation model that can focus on high-frequency and detailed information. However, most representation-based models assume that the same representations are shared by the source input and the target output, limiting a particular style’s local structures in the synthesis process. To relax this constraint, Wang *et al.* [65] introduced a semi-coupled dictionary learning method, in which a linear transformation is used to bridge the gap between two different domain-specific representations. Gao *et al.* [7] also took a two-step algorithm [63] into consideration, presenting a selection scheme to generate the initial pseudo-images and introducing a

sparse-representation-based enhancement (SRE) to synthesize sketches.

2.2.4 Combination Models

Recently, some works are to explore the combination models, which combine different machine learning models, *e.g.*, combining Bayesian inference and subspace learning methods. Berger *et al.* [8] proposed a model to simulate the styles of the different artists and the process of abstraction, which can be used for facial-sketch synthesis. Song *et al.* [66] introduced a real-time FSS method, which first uses a k-NN algorithm to find the top-k similar local patches. Then uses a linear combination to compute the corresponding sketch image and finally uses image denoising technology to enhance the visual quality. However, the model [66] is still time-consuming due to the k-NN process, so Wang *et al.* [67] addressed this problem by replacing offline random sampling with an online scheme that is further combined with a recognition weight representation. Most existing traditional methods are entirely dependent on the scale of the training data, so Zhang *et al.* [68] presented a robust model trained on a template stylistic sketch. The model includes representation learning, MRF, and a cascaded model. Li *et al.* [69] proposed a free-hand sketch synthesis method, combining a perceptual grouping model with a deformable stroke model. The work in [70] introduces an adaptive learning method that combines representation learning and a Markov network. Men *et al.* [71] proposed a common framework for interactive texture transfer with structure guidance. Their model implements the synthesis process dynamically using multiple channels, including structure extraction, structure propagation, and guided texture transfer.

2.3 General Image Synthesis

Deep facial-sketch synthesis belongs to the task of image generalization. Therefore, general image synthesis methods, like image-to-image translation and neural style transfer, can also be used to generate facial sketches. We will overview various cutting-edge transformation models.

2.3.1 Image-to-Image Translation

Image-to-image translation (I2I) [72] is a hot topic in computer vision and machine learning. The goal

is to transform the input image from a source domain to a different target domain while retaining the intrinsic source content and transferring the extrinsic target style. Current I2I models are typically built on a generative adversarial network (GAN) [73]. They can be generally categorized into supervised and unsupervised I2I.

Supervised I2I. Supervised I2I uses aligned image pairs as the source and target domain to learn a transformation model that can convert the source image into the target image. One representative I2I method is Pix2pix [31], which applies a conditional GAN (cGAN) [74] to the task. The main difference from the original cGAN is that the generator in Pix2pix is a U-Net [75]. However, Wang *et al.* [23] observed that the adversarial training in Pix2pix is unstable, preventing the model from generating high-resolution images. Therefore, they extended the original Pix2pix with a new feature matching loss, which can generate high-resolution images of size 2048×1024 . Zhu *et al.* [76] proposed the BicycleGAN, which includes a conditional VAE and a conditional latent regressor GAN, to resolve the collapse problem and achieve improved performance. Further, to reduce the loss of semantic information in the Pix2pixHD model [23], Park *et al.* [24] introduced a SPADE-based generator, which adds spatially-adaptive normalization into the generator of Pix2pixHD so as to enhance the semantic information throughout the network.

Unsupervised I2I. Collecting paired data is not practical because it is labor-intensive. Therefore, several unsupervised I2I models have been proposed to train two different generative networks under the constraint of a cycle-consistency loss. If we convert a zebra image to a horse image and then back to a zebra image, we should get the same input image back. Examples include CycleGAN [21], DiscoGAN [77], and DualGAN [78]. Later, Liu *et al.* [22] proposed an unsupervised I2I model (UNIT), in which the same latent code in shared latent feature space can represent image pairs in different domains. Kim *et al.* [30] later proposed a novel attention module with a new normalization function, which they integrated into a GAN model to supervise texture and shape variations flexibly. By rethinking the standard GAN model, Chen *et al.* [26] proposed a NICE-GAN with the key idea of coupling

discriminators and encoders, *i.e.*, reusing the discriminator parameters for encoding the input. Zhao *et al.* [79] proposed ACL-GAN, which utilizes a new adversarial consistency loss instead of a cyclic loss to emphasize the commonality between the source and target domains. To improve the content representation ability, Chang *et al.* [25] proposed DMAP to leverage the relationship between content and style. Specifically, the model maps content features from a shared domain-invariant feature space into two separate domain-specific ones. Further, DRIT++ [27] uses two image generators, two content encoders, a content discriminator, two attribute encoders, and two domain discriminators to embed an image into a domain-invariant content space and a domain-specific attribute space. Besides, Jiang *et al.* [80] proposed two-stream I2I translation (TSIT) to learn both semantic structural features and stylistic features and then fuse the feature maps of the content and style in a coarse-to-fine manner. More recently, Zhang *et al.* [81] proposed a CoCosNet for exemplar-based image translation, which contains two sub-networks. The first embeds the inputs from different domains into a feature domain that depends on the semantic correspondence. Meanwhile, the second uses a series of denormalization blocks to synthesize the target images progressively. Zhou *et al.* further extended the CoCosNet with full-resolution semantic correspondence learning [82], with the main difference being the use of a regular and GRU-based propagation applied iteratively at each semantic level. More recently, Chen *et al.* [83] proposed a SofGAN, which decouples the portrait feature into a geometric feature and a texture feature. These two features are then fed into two network branches. The first branch is a hyper network to decode the geometric feature into the weight of the SOF net that represents the semantic occupancy field (SOF) among 3D space. Then, a segmentation map is rendered via a ray-casting-marching scheme using the SOF net's output features. The second branch is a texture transformation of each semantic region using a GAN generator with a style code sampled from the texture space. Finally, a novel Semantic Instance Wise (SIW) StyleGAN module is used to stylize the generated segmaps and output a photorealistic portrait regionally.

2.3.2 Neural Style Transfer

Neural style transfer (NST), which aims at generating visually appealing images via neural networks, has been introduced into the FSS task [84]. Specifically, NST is used to render a content image in different styles. NST methods can be categorized into optimization-based methods and model-based methods.⁴

Optimization-based methods. The online NST algorithm iteratively updates a given input image to match the desired CNN features, including the photo's content and artistic style information. Gatys *et al.* [87, 88] made the first contribution to this field, using a classical CNN (*i.e.*, VGG [89]) to render an image with famous painting styles. Besides, StyleGAN [90] uses a latent space to maintain consistent results for image synthesis. However, it is challenging to achieve promising results under the given conditions. Recently, Abdal *et al.* [91] integrated the classical NST [87, 88] into the StyleGAN model, using NST to project the input image into the latent space defined in StyleGAN. Then, Kotovenko *et al.* [92] further enhanced the classical NST [87, 88] by optimizing parameterized brushstrokes, which is built on a simple differentiable rendering mechanism.

Model-based methods. Optimization-based online methods achieve satisfactory results, but there are still some limitations. One major drawback is the slow computational speed and high cost of online iterative optimization. To address this issue, several works introduce a feed-forward network to mimic the optimization objective of style transfer [84].

End-to-end models can be divided into those that design a basic deep neural architecture and those that introduce a new loss function. For basic architectures, Johnson *et al.* [93] took advantage of the benefits of the neural network and optimization-based NST model and proposed a method for training a feed-forward network using a new perceptual loss. TextureNet [94] follows a similar idea but with different neural network

architecture. Both [93] and [94] are real-time style transfer methods. Chen and Schmidt [95] introduced a style swap operation to exchange the patches with visual context and those with style, further formulating a new optimization objective that aims to learn an inverse neural network for arbitrary style transfer. In terms of methods based on loss function, CartoonGAN [85] was presented to transfer real-world photos into cartoon-style images. It consists of two novel loss functions designed to preserve clear edge information and cope with the stylistic difference between photos and cartoons.

Recently, several researchers have begun using a small number of parameters to characterize each style, *i.e.*, changing the parameters in the normalization layer for style transfer. Dumoulin *et al.* [96] made the exciting observation that normalization layers can reflect the statistical properties of different styles. Therefore, they scaled and shifted the parameters in these layers while keeping the convolutional parameters unchanged to obtain better NST. Further, they introduced flexible conditional instance normalization, enabling style transfer by simply changing the normalization parameters online. Ulyanov *et al.* [97] improved their previous TextureNet [94] by simply applying normalization to each image rather than a batch of images, which they called instance normalization. Moreover, they also demonstrated that the style transfer network with instance normalization could converge faster than that with batch normalization while achieving visually better results. Later, Huang and Belongie [98], following a similar idea, introduced adaptive instance normalization into the GAN model, aligning the content and style features. Li *et al.* [99] further used the first few layers of a pre-trained VGGNet [89] to extract the feature representation. However, they replaced the AdaIN layer with whitening and coloring transformations, enabling the universal style transfer. Similar to I2SGAN [91], Richardson *et al.* [86] improved the classical StyleGAN with a novel encoder network that learns many style vectors that are fed into a pre-trained generator, forming an extended $\mathcal{W}+$ latent space.

2.4 Deep Photo-Sketch Synthesis

Deep photo-sketch synthesis is a recent branch of the FSS task, in which deep learning is used

⁴Note that some related works belong to the general GAN-based model, such as CartoonGAN [85] and pSp [86]. These GAN models can be used for either neural style transfer or image-to-image translation. Since we don't make a specific review of the generalized GAN model, we classified a few GAN models into the neural style transfer task as a quick overview of these methods.

Table 2 Summary of popular related works. These can be categorized into three types: *Traditional Facial Synthesis*, *General Image Synthesis*, and *Deep Image-to-Sketch Synthesis*. **Publ.:** Publication information. **Year:** Publication year. **Code:** The link of the corresponding open resources. **Component:** The key components of each model. **Dataset:** A = TU-Berlin Sketch Dataset [100], B = Disney Portrait Dataset [8], C = FERET [101], D = AR [33], E = Self-Collected, F = MSCOCO [102], G = ImageNet [103], I = CelebA [28], L = DTD [104], P = Wikiart [105], Q = Cityspace [106], R = CMP Facades [107], S = Edge2photo [108, 109], U = Day2night [110], V = MNIST [111], Y = CUFS [1], Z = Caltech-200 Bird [112], AC = CelebAHQ [113], AD = NYU Indoor RGBD dataset [114], AE = ADE20K [115], AG = FERET [35], AK = QMUL-Shoe-Chair-V2 [116], AL = QuickDraw dataset [117], AP = Yosemite [21], AQ = cat2dog [27], AR = Flickr Landscapes [24], AS = APDrawing Dataset [2], AT = Anime Faces of Getchu [118], AU = Selfie2anime [30], AV = hourse2zebra [21], AW = photo2vangogh [21], AX = photo2portrait [27], BH = Berkeley Deep Drive [119], BI = SYNTHIA dataset [120], BJ = UPDG [9], BK = DeepFashion [121], BU = FFHQ [90], BV = DIV2K [122], BW = LHI [123], BX = VIPSL [6], BY = IIIT-D [4], BZ = Map2Aerial [31], CB = StanfordCars [124], CH = LSUN [125], CU = CUFSF [5]. **Assist.:** Assistant Information, *e.g.*, Bm.= Background map, Sm.= Segmentation map, Fl. = Facial landmark, Sv. = Style vector, Cm. = Color map, Attr. = Facial Attribute, Km. = Keypoint map, Tp. = Texture patch. **Cite.:** Google citation statistics are from 2022-05-21.

#	Model	Publ.	Year	Code	Component	Dataset	Assist.	Cite.
Traditional Facial Synthesis								
1	EFSGNS [45]	ICCV	2001	-	Active Shape Model, Non-parametric Sampling	E	-	160
2	Nonlinear [59]	CVPR	2005	-	Local Linear Preserving, Eigentransform	Y	-	398
3	E-HMM [47]	TCSVT	2008	-	Embedded Hidden Markov Model, Selective Ensemble	Y	-	165
4	HCM [48]	PAMI	2008	-	Graph, Minimum Description Length	C, D, BW, E	-	93
5	MRF [1]	PAMI	2009	Code	Multi-scale Markov Random Fields	Y	-	872
6	LPR [49]	ECCV	2010	-	Local Evidence Function, Patch Matching, Shape Prior, MRF	Y	-	120
7	LRM [61]	ICIG	2011	-	Local Regression, kNN	Y	-	19
8	MOR [62]	HCH	2011	-	Multivariate Output Regression	Y	-	22
9	MDSR [6]	ICIG	2011	-	LLE, Dictionary Learning, Sparse Representation	Y, BX	-	55
10	SVR [63]	ICIP	2011	-	Support Vector Regression	Y, BX	-	41
11	SCDL [65]	CVPR	2012	-	Sparse Coding, Semi-coupled Dictionary Learning	Y	-	613
12	MWF [50]	CVPR	2012	-	Markov Weight Fields, Cascade Decomposition	Y, E	-	173
13	SR [7]	TCSVT	2012	-	Sparse Neighbor Selection, Sparse-Representation Enhance	Y, BX	-	185
14	SAPS [8]	TOG	2013	-	Edge Detection, Shape Deformation	B	-	116
15	FESM [51]	BMVC	2013	-	Markov Random Field, Graph-cut	E	-	22
16	Transductive [52]	TNNLS	2013	-	Probabilistic graph model, Transductive Learning	Y, CU	-	167
17	CDFSL [60]	ICCV	2013	-	Coupled Dictionary and Feature Space Learning	Y	-	177
18	REB [66]	ECCV	2014	Project	kNN, Linear Estimation, Sketch Denoising	Y, D	-	124
19	RobustStyle [68]	TIP	2015	-	Sparse Representation, Multi-scale Selection	Y, E	-	49
20	SPP [53]	TCSVT	2015	Project	Superpixels, Markov Networks	Y, CU, BY	-	45
21	MR [54]	TNNLS	2016	-	Markov Networks, Edge Enhancement, Alternating Opt.	Y, BY	-	107
22	DSM [69]	IJCV	2017	Project	Perceptual Grouping, Deformable Stroke Model	A, B	-	37
23	AR [70]	NC	2017	-	Adaptive Representation, Markov Networks	Y	-	10
24	RS [67]	PR	2018	-	Offline Random Sampling, Locality Constraint	Y, CU	-	96
25	CFITT [71]	CVPR	2018	Github	PatchMatch, Guided Texture Transfer	E	Sm.	19
General Image Synthesis								
26	NST [87, 88]	CVPR	2016	Github	Parametric Texture Mode, Representation Inversion	E	-	3853
27	FNS [93]	ECCV	2016	Github	Image Transformation and Loss Network, Perceptual Loss	F	-	7038
28	TextureNet [94]	ICML	2016	Github	Generator Network, Descriptor Network,	E	-	813
29	FPST [95]	NeurIPS	2016	Github	CNN, Style Swap, Inverse Network	F, P	-	285
30	CIN [96]	ICLR	2017	Github	Conditional Instance Normalization	G, E	-	838
31	ITN [97]	CVPR	2017	Github	Instance Normalization, Julesz Generator Network	E	-	546
32	AdaIN [98]	ICCV	2017	Github	Adaptive Instance Normalization	F, P	-	2123
33	WCT [99]	NeurIPS	2017	Github	Multi-level Stylization, Whitening and Coloring Transforms	F, L	-	578
34	CartoonGAN [85]	CVPR	2018	Github	GAN, Semantic Content Loss, Edge-promoting Loss	E	-	227
35	I2SGAN [91]	CVPR	2019	Github	StyleGAN, Embedding	AC, BU	-	389
36	RST [92]	CVPR	2021	Github	Differentiable Renderer, Brushstrokes Parameterization	E	-	10
37	pSp [86]	CVPR	2021	Github	StyleGAN, Disentangled Latent Feature, Map2Style	AC, BU	-	194
38	Pix2pix [31]	CVPR	2017	Github	Generator with Skip, PatchGAN	A, G, Q, R, S, U, BZ	-	13244
39	CycleGAN [21]	ICCV	2017	Github	Map Functions and Discriminators, Cycle Consistency Loss	A, G, Q, R, S, U, AV, AW	-	12734
40	DualGAN [78]	ICCV	2017	Github	Trained in Closed Loop, Reconstruction Loss	R, U, Y, CU, BZ, E	-	1554
41	DiscoGAN [77]	ICML	2017	Github	GAN with a Reconstruction Loss	CI, K, I, AH, S	-	1714
42	BicycleGAN [76]	NeurIPS	2017	Github	cVAE-GAN, cLR-GAN	R, S, U, BZ	-	1114
43	UNIT [22]	NeurIPS	2017	Github	Common Latent Space, VAEs, Cycle-consistency, GAN	G, I, Q, V, W, X, BI	-	2138
44	Pix2pixHD [23]	CVPR	2018	Github	Coarse-to-fine Generator, Multi-scale Discriminator	Q, AD, AE, AF	-	2527
45	MUNIT [126]	ECCV	2018	Github	Content/Style Encoder, AdaIN, Decoder	A, S, AP, BI, E	-	1615
46	SPADE [24]	CVPR	2019	Github	Spatially-Adaptive Normalization, Pix2pixHD	F, Q, AE, AR	Sm.	1362
47	U-GAT-IT [30]	ICLR	2020	Github	Attention map, Adaptive Layer-Instance Normalization	AU, AV, AW, AX	-	248
48	CoCosNet [81]	CVPR	2020	Github	Cross-domain Correspondence, Translation Network	AE, AC, BK	-	104
49	TSIT [80]	ECCV	2020	Github	Multi-scale Feature Normalization, Two-stream Network	Q, AE, AP, AW, BH	-	34
50	DSMAP [25]	ECCV	2020	Github	Domain-specific Content Mappings	AQ, AW, AX	-	13
51	ACL-GAN [79]	ECCV	2020	Github	Adversarial Consistency Loss, MUNIT	I, AU	-	29
52	DRIT++ [27]	IJCV	2020	Github	Disentangled Representation with Cross-cycle Consistency	AP, AQ, AW, AX, I	-	218
53	CoCosNetV2 [82]	CVPR	2021	Github	ConvGRU Module, Hierarchical Strategy, PatchMatch	AE	-	32
54	SofGAN [83]	TOG	2022	Project	SOF Net, StyleGAN, Style Mixing, SPADE	AC, BU, I	Bm., Sm., Attr.	11

Table 3 Summary of popular related works. Please refer to Table 2 for more detailed descriptions.

#	Model	Publ.	Year	Code	Component	Dataset	Assist.	Cite.
Deep Image-to-Sketch Synthesis								
55	FCRL [127]	ICMR	2015	-	Fully Convolutional Network	Y	-	127
56	DGFL [128]	IJCAI	2017	-	Deep CNNs, Graphic model	Y	-	34
57	Scribbler [129]	CVPR	2017	Project	Encoder-decoder with residual connections, GAN	Y, E	-	427
58	FSSC2F [130]	AAAI	2018	-	U-Net, Probabilistic Graphic Model	Y	-	11
59	TextureGAN [131]	CVPR	2018	Github	Local Texture Loss, VGG Loss, Scribbler	E, S	Bm. Tp.	221
60	SCC-GAN [132]	CVPR	2018	Code	Hybrid model, Shortcut Cycle Consistency	AK, AL	-	76
61	ContextualGAN [133]	ECCV	2018	Github	Contextual Loss, Joint Representation, GAN	I, Z, CB	-	74
62	pGAN [134]	IJCAI	2018	Github	UNet, Parametric Sigmoid, CycleGAN	Y, CU	Bm.	24
63	MRNF [135]	IJCAI	2018	-	Markov Random Neural Fields	Y	-	16
64	PSS ² -MAN [136]	FG	2018	Github	Multi-Adversarial Networks, CycleGAN	Y, CU	-	98
65	DualT [137]	TIP	2018	-	Deep Features, Intra- and Inter-Domain Transfer	Y	-	51
66	MDAL [11]	TNNLS	2018	Github	Domain alignment, Interpreting by Reconstruction	Y, CU	-	45
67	FAG-GAN [138]	WACVW	2018	-	Attribute Classification, Conditional CycleGAN	I, AG	-	30
68	Geo-GAN [139]	BIOSIG	2018	Github	Geometry Discriminator, CycleGAN	CU, AG	-	17
69	PI-REC [140]	arXiv	2019	Github	Coarse-to-Fine, LSGAN, VGG Loss	A, I, S, AT	Cm.	18
70	DLLRR [141]	TNNLS	2019	-	Coupled Autoencoder, Low-rank Representation	Y	-	27
71	Col-cGAN [142]	TNNLS	2019	-	Collaborative Loss, cGAN, Deep Collaborative Nets	Y, CU	-	43
72	CFSS [143]	TIP	2019	-	cGAN, VGG, Feature Selection	Y	-	14
73	KT [144]	IJCAI	2019	-	Knowledge Transfer, Teacher-Student Net	Y, CU	-	16
74	im2pencil [145]	CVPR	2019	Github	Outline and Shading Branch Networks, Pix2pix	E	Sv.	28
75	ISF [146]	ICCV	2019	Project	Shape and Appearance Generators, Two-stage	S, AC, E	-	62
76	APDrawing [2]	CVPR	2019	Github	Hierarchical GAN, DT Loss, Local Transfer Loss	AS	Fl., Bm., Sv.	82
77	APDrawing++ [10]	TPAMI	2020	Github	APDrawing, Line Continuity Loss	AS	Fl., Bm., Sv.	12
78	UPDG [9]	CVPR	2020	Github	Asymmetric CycleGAN, Cycle-consistency Loss	BJ	Fl., Bm., Sv.	22
79	WCR-GAN [147]	CVPR	2020	Github	Cartoon Representation Learning, GAN	F, BU, BV, E	-	29
80	EdgeGAN [148]	CVPR	2020	Project	SketchyCOCO, Divide-and-Conquer strategy	F	Attri.	34
81	DeepPS [149]	ECCV	2020	Github	Sketch Refinement with Dilations, Pix2pixHD	AC, I	-	25
82	DeepFaceDrawing [150]	TOG	2020	Github	Component Embedding, Feature Mapping, Image Synthesis	AC, E	Km.	41
83	CA-GAN [151]	TC	2020	Github	Composition/Appearance Encoder, P-Net, Stacked GAN	Y, CU	Fl.	44
84	IDA-CycleGAN [152]	PR	2020	-	CycleGAN, Identity Loss, Recognition Model	Y, CU	-	41
85	IPAM-GAN [153]	SPL	2020	-	Identity-preserved Adversarial Model, U-Net	Y, CU	-	12
86	MvDT [154]	TIP	2020	Github	CNN [89] Features, Hand-crafted Features	Y, E	-	10
87	MSG-SARL [155]	TIFS	2021	-	Self-attention Residual Learning, Multi-scale Gradients	Y, CU	-	6
88	GANSketching [156]	ICCV	2021	Project	Weight Adjusting, Cross-domain Fine-tuning	CH, AL	-	8
89	DoodleFormer [157]	Arxiv	2021	-	Transformer, Part Locator and Part Sketcher Networks	CK	-	1

to improve performance and quality. The related works can be divided into three categories. The first aims to translate any sketch images into their corresponding RGB images. The second tries to convert any RGB images into sketch images. The last mainly focuses on facial-sketch synthesis.

General Sketch-to-Image. Xian *et al.* [131] proposed the TextureGAN model to synthesize an image under the supervision of a sketch, color, and texture. TextureGAN consists of a ground-truth pre-training module and an external texture fine-tuning part. Then, Lu [133] *et al.* introduced a two-stage contextual GAN to achieve sketch-to-image generation. This framework trains a classical GAN model with a newly defined loss, representing the joint distribution and capturing the inherent relation between a sketch and its corresponding image. Inspired by image in-painting [158], You *et al.* [140] proposed the PI-REC model, which contains three phases: an imitation phase, generating phase, and refinement phase. PI-REC is progressively trained using only one generator and one discriminator. The ISF introduced in [146] is a gating-based approach, which allows a single generator to be used to generate distinct classes without feature mixing. Recently, Gao *et al.* [148]

proposed EdgeGAN for object-level image synthesis given freehand scene sketches. This framework contains two sequential modules: foreground generation and background generation. Yang *et al.* [149] presented a deep plastic surgery model to simulate the coarse-to-fine painting process of human artists. Chen *et al.* [150] proposed a local-to-global framework to allow any user to produce high-quality face images. Their model consists of three modules: a component embedding, a feature mapping, and an image synthesis.

General Image-to-Sketch. Song *et al.* [132] proposed the first deep stroke-level photo-to-sketch synthesis method, which is a hybrid model with a shortcut cycle consistency constrained by a VAE-style reconstruction loss. As the default setting of I2I and NST, both can synthesize artistic portrait drawing (APD) images. However, they do not meet practical requirements because APD images usually have a highly abstract style and graphic elements. Therefore, Yi *et al.* [2] proposed an APDrawing to transform an input face image into its corresponding APD image, in which a hierarchical GAN model is built by combining both a global and a local network. Then, they further proposed an APDrawing++ [10], in which they

used an auto-encoder to refine the subtle facial features and presented a novel line continuity loss to enhance the line continuity of APDrawing. However, both of these APDrawing methods require pair-wise data for training. To handle this problem, Yi *et al.* thus proposed an asymmetric cycle-structure GAN [9], which contains a relaxed forward cycle consistency loss (*a.k.a.* truncation loss) to prevent the reconstructed photo from being noisy, and a strict cycle consistency loss to enhance the performance. This method also uses multiple local discriminators to ensure the quality of the facial portrait drawings. Different to portrait drawing, Wang *et al.* [147] observed the behavior and properties of cartoon paintings and proposed three different representations considering surface, texture, and shape information, respectively. In addition, they also released the new SketchyCOCO dataset to better train and evaluate the performance of their model. Based on Pix2pix, Li *et al.* [145] designed a two-branch network (called im2Pencil) to implement photo-to-pencil translation, which can simulate sketch outlines and shadows. Wang *et al.* [156] presented a GAN sketching method to rewrite GAN with one or more sketches. This new method uses regularizations to preserve the original GAN’s diversity and image quality while matching the generated sketch images with users’ needs through a cross-domain adversarial loss. Bhunia *et al.* [157] introduced a new transformer architecture to generate various yet realistic creative sketches consisting of two networks. The first part of locator networks aims to capture the coarse structure by observing the relationship between local patterns. And the second part sketcher network, follows the standard GAN, which aims to synthesize high-quality sketch images..

Photo-Sketch Synthesis. Zhang *et al.* [127] were the first to use a fully convolutional neural network (FCNN) to build a deep photo-to-sketch synthesis model. Then, the works [108, 130, 135] integrated deep features into probabilistic graph model learning, achieving better performance than traditional models [1, 50]. To make the network more flexible, Zhang *et al.* [134] took the key idea of CycleGAN and proposed a novel pGAN, which uses a special parametric Sigmoid activation function to reduce the effects of photo priors and illumination variations. To improve the quality of the

generated photo/sketch, Wang *et al.* [136] introduced a synthesis method using multi-adversarial networks (PS²MAN). Their model uses two U-Nets to generate high-quality images from low to high resolution. To achieve the same goal, Zhang *et al.* [11] further proposed a facial-sketch synthesis by multi-domain adversarial learning (MDAL), which overcomes the defects of blurs and deformations. The basic idea behind MDAL is the concept of “interpretation through synthesis”, which is built upon two diverse generators. Kazemi *et al.* [138, 139] proposed an improved version of CycleGAN, which focuses on the facial attributes during the portrait synthesis process. Zhang *et al.* [141, 143] introduced two methods by combining an auto-encoder and traditional subspace learning, which is more effective than the traditional FSS methods. Besides, Zhu *et al.* [142] proposed a collaborative framework that exploits the interaction information of two opposite generators by introducing a collaborative loss. However, it is difficult to train a good model due to the lack of large-scale training data. Therefore, Zhu *et al.* [144] proposed to use classical knowledge distillation to learn two well-defined student mapping networks via two strong teacher networks. More recently, the works in [152, 153] introduced identity-aware models, which use a new perceptual loss to train a better image generative model, and thus consider the downstream task, *e.g.*, face recognition, as the final goal. Yu *et al.* [151] proposed a new composition-assisted generative adversarial network, which helps synthesize realistic facial sketches/photos by using facial composition information. By leveraging the relationships between features, [155] implemented a multi-scale self-attention residual learning framework for face photo-sketch conversions. Finally, the method proposed in [154] does not need any images from the source domain for training, enabling it to leverage both deep features (extracted from the CNN) and handcrafted features flexibly.

3 Proposed FS2K Dataset

In this section, we introduce the proposed FS2K. Some example images are shown in Fig. 2. We describe FS2K in terms of two key aspects, namely dataset collection, and data annotation. Overall, FS2K includes 2,104 photo-sketch pairs, which are

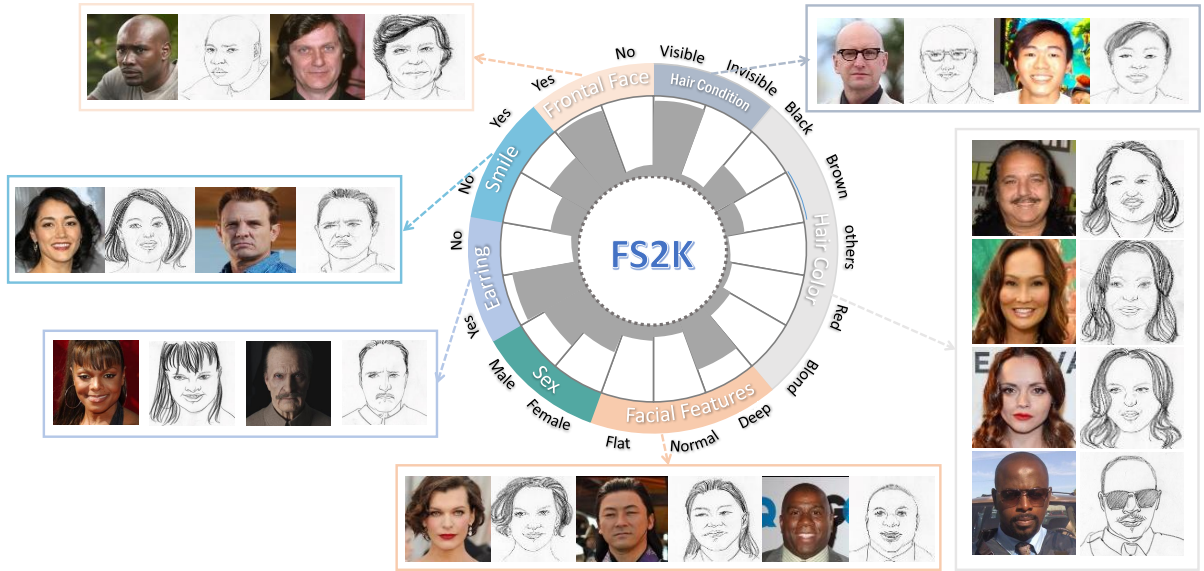


Fig. 4 Statistics and examples from the FS2K dataset. Please refer to Sec. 3 for details.

split into 1,058 for training and 1,046 for testing. The complete dataset is available at <https://github.com/DengPingFan/FS2K>.

3.1 Data Collection

To establish a long-lasting benchmark, the data should be carefully selected to cover diverse scenes from different views, such as lighting conditions, skin colors, sketch styles, and image backgrounds. To this end, we introduce FS2K, a new high-quality dataset⁵ for the FSS task.

Our FS2K includes 2,104 photos from real scenes, the Internet, and other datasets. The majority, however, come from CASIA-WebFace [159], which is a large-scale (*i.e.*, 500K images) labeled dataset of faces in the wild. CASIA-WebFace was collected from the IMDb⁶ website and contained well-organized information, such as name, gender, and birthday. Thanks to the rich and clean open-source data from CASIA-WebFace, it could be used to build our high-quality and representative benchmark. We manually selected 1,529 images to cover a large span of major challenges faced in realistic scenes, such as varying background, hairstyle (*e.g.*, long, short), accessories (*e.g.*, glasses, earrings), and skin information (*e.g.*, patch image on a given face).

Because the photos selected in CASIA-WebFace are taken from a single angle, multi-angle face images for the same person are missing. To this end, we invited eight actors to take 98 photos under different settings (*e.g.*, lighting conditions, face angles). In addition, to further increase the diversity, we also collected some children's photos and some faces with smaller face-to-image ratios. The remaining 477 face photos come from other free stock photos websites, including Unsplash,⁷ Pexels,⁸ Pngimg,⁹ and Google.

3.2 Data Annotation

There are four types of annotations in our FS2K, including sketch drawing, sketch style, color, and contour feature annotations.

3.2.1 Sketch Drawing

Participants. Three senior artists (including two male and one female) from the Sichuan Fine Arts Institute were hired to participate in the study.¹⁰ All three participants had normal or corrected to normal vision. None of the participants suffered

⁵This dataset is for scholarly communication only.

⁶<http://www.imdb.com>

⁷<http://www.unsplash.com>

⁸<http://www.pexels.com/>

⁹<http://pngimg.com/>

¹⁰The <https://www.scfai.edu.cn/english/> is one of the four most prominent art academies in China. The three senior artists are all from the Design Academy.

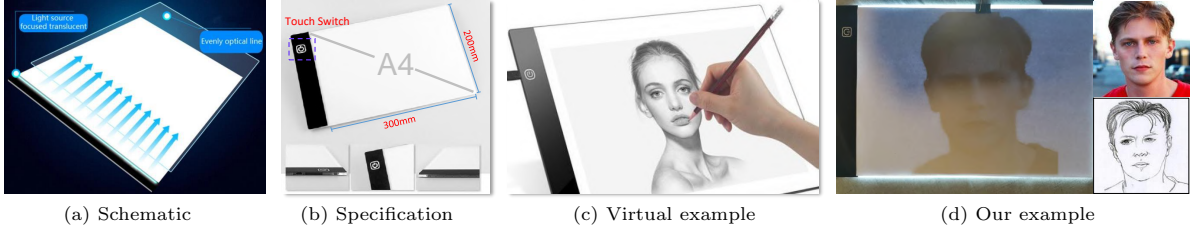


Fig. 5 Use of the copy table and an example. Zoom-in for the best view. See Sec. 3.2 for more details.

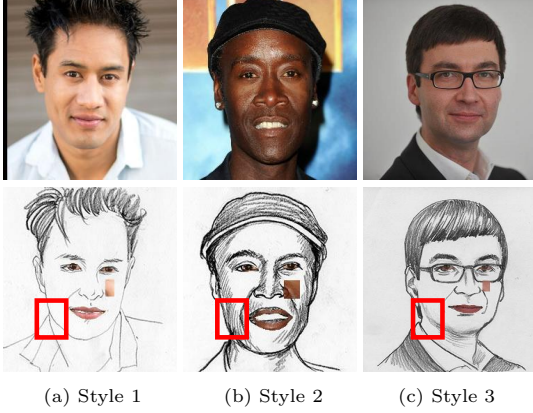


Fig. 6 Three sketch styles in our FS2K. As shown in the cheek region, the styles include simple lines (style 1), long strokes (style 2) and repeated wispy details (style 3).

color-blindness or color-weakness. The participants ranged in age from 20 to 23 years, with an average of five years of professional experience in sketch drawing.

Apparatus. The three artists drew all sketch images with the assistance of a Copy Table LED Board.¹¹ Fig. 5 shows the copy table we used and an example (Fig. 5-d) of a face sketch drawn by our artists. The touch switch region in our device supports three levels of adjustable brightness, so the artists can use the button to change the brightness they desire. This helped them locate the contours of facial features according to the photo information from the bottom of the LED board. Moreover, this equipment also helped to ensure content similarity and face alignment between sketches and corresponding photos. At the same time, the drawings retain the artist’s sketch style.

¹¹Fig. 5-a presents the copy table, which has an LCD backlight. It requires a high voltage input of 100 ~ 240V and 0.6A working current. Its size is A4 (*i.e.*, 300 × 200 × 3.5mm) in Fig. 5-b, and the luminous intensity is 300 ~ 350LM. Therefore, it has become the most popular copy table product, after the aluminum alloy copy table, for animators (see Fig. 5-c).

3.2.2 Sketch Style Annotation

Our FS2K contains three different styles, which enrich the diversity of sketches, as shown in Fig. 6. This enables different artists’ skills to be captured while making FS2K more challenging than previous FSS datasets.

We created a balanced dataset to facilitate the comparison of different methods, *i.e.*, the number of the images with the three different styles are equally distributed. Specifically, in the training set, the samples with style1, style2, and style3 are 357, 351, and 350, respectively. In the test set, they are 619, 381, and 46, respectively.

3.2.3 Facial Feature Annotation

Sketches are rapidly executed freehand drawings, which have less attribute information than the original images, *e.g.*, facial texture, facial expressions [160], facial posture, *etc.* Therefore, it is challenging to restore real images (*i.e.*, S2I task) based on a single sketch image. Meanwhile, in real-world applications, we can use auxiliary facial information (such as gender, accessories, and hairstyle) to narrow down a suspect in a database. Following [161], we added some additional facial feature annotations, including *gender*, *smile*, *face pose*, *hair condition*, *hair color*, *earring*, and *skin texture*. We hired two data annotators to label all photos and performed cross-checking to ensure the accuracy of the final annotations. Overall labels can be found in Table 4, while the details of each are described below.

Gender. Gender is a high-level human attribute commonly used in traditional face databases such as CelebA [28] and LFW [162]. It has been extensively studied in face detection and recognition [163–165]. Therefore, we carefully labeled all photos in FS2K with gender attributes. Specifically, there are 574 male photos and 484 female photos in the training set, and 632 male photos and 414 female photos in the test set.

Table 4 Number of images for each attribute in the training and test datasets.

FS2K (Ours)	w/ H	w/o H	H(b)	H(bl)	H(r)	H(g)	M	F	w/ E	w/o E	w/ S	w/o S	w/ F	w/o F	S1	S2	S3
Train	1010	48	288	423	60	239	574	484	209	849	645	413	917	141	357	351	350
Test	994	52	290	418	44	242	632	414	187	859	670	376	872	174	619	381	46

Smile. Smiling is a primary human activity that represents a positive emotional state. As such, many studies have focused on smile detection [166, 167] or used smile as an attribute for recognition [168]. Therefore, we also consider a smile a key attribute in our dataset. Specifically, the training set contains 645 smiling people and 413 with no obvious expression, while the test set contains 670 smiling people and 376 with no expression. We make sure that the proportion of smiling people in the training and test sets is as close as possible.

Face Pose. The facial attributes may cover only a small part of the image, but the photo is usually dominated by the effects of pose [169]. Moreover, pose will affect the performance of face recognition [170], tracking [171], and synthesis [172]. Therefore, the facial pose is useful auxiliary information. We define a portrait with the head rotated within 30 degrees as a frontal face pose. According to this definition, the training set has 917 frontal photos, while the test set has 872. The remaining have side face poses.

Hair Status and Color. Hair is a saliency feature of the head that may change in different situations. Even if there is sufficient information in the internal features of the face for recognition, manipulating the hair can harm the performance [173, 174]. Moreover, facial synthesis and retrieval systems often use hair as an important cue [175, 176] to improve the quality of generated images. For FSS, although the sketches contain the hair contour, the corresponding color information and hair status (with or without hair) are missing. Therefore, in FS2K, we provide annotations of the hair status, which includes four available colors (*i.e.*, black, brown, red, and blond) and another status (*i.e.*, bald or wearing a hat), as shown in Fig. 4. In other words, for faces with hair, we mark the color information directly, while cases of thinning hair or wearing a hat are marked as separate attributes. The statistical results of this annotation can be found in Table 4.

Earrings. The simplified characteristics of sketch drawings lead to unclear earring contours. Meanwhile, as shown in Fig. 4, earrings in real

photos are visible. Therefore, in FS2K, we provide annotations for whether or not earrings are present, which can help the model training. Specifically, the training set has 209 people with earrings, and the test set has 187.

Skin Texture. Skin texture provides a large amount of detailed local information and is used as a vital feature for face recognition [177, 178]. However, this critical information is completely lost in sketch images. Therefore, we clip a small patch from the real photo and use it as the skin texture, as shown in Fig. 6. We also include the average RGB value for the corresponding lip and eyeball region to provide more information for future research.

4 Proposed FSGAN Baseline

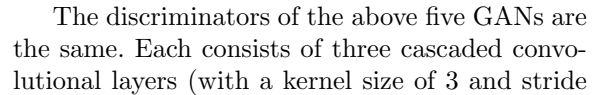
4.1 Problem Definition

Facial synthesis (FS) aims to generate target representations of human faces based on the given inputs. This process can be formulated as $X_o = F(X_i)$, where X_i and X_o denote the input and output (*e.g.*, RGB images and sketches) of facial representations F indicates the synthesis function. In this paper, based on the overall architecture of [2, 10], we design the baseline, FSGAN, for both the I2S task¹² and S2I task¹³ inspired by pix2pixHD [23]. Instead of focusing on direct image-level facial synthesis, we propose a two-stage “bottom-up” facial synthesis architecture, as shown in Fig. 7. Hence, our FSGAN consists of two cascaded stages built upon multiple generative models (*i.e.*, GANs).

The first stage is comprised of five parallel GANs, which are designed to synthesize the local facial components separately. Given an input, four facial regions (*e.g.*, left eye, right eye, nose, and mouth) and the rest of the inputs are cropped and fed into their corresponding GANs in the first stage for synthesizing key facial features. These synthesized facial component patches are

¹² $X_{ske} = F(X_{img}, X_{style})$, where X_{style} denotes the sketch style of input.

¹³ $X_{img} = F(X_{ske})$.



of 2) followed by global average pooling. Then, a 1×1 convolutional layer and a sigmoid function are used to predict the probability of the generated results being real or fake.

Based on the above design, the first stage of FSGAN can restore details of the facial components in both the I2S and S2I tasks. At the end of this stage, the synthesized patches are stitched together to restore the intact facial synthesis result X_{intact} . Since different generators synthesize the patches, their overall appearances are inconsistent, which becomes even more obvious in the stitched result. To this end, the stitched result is then fed to the next stage to adjust and refine the global structure and appearance.

4.3 Facial-Sketch Synthesis

To address the inconsistency issue of the output from the first stage, we introduce the second stage, which is designed as another GAN model inspired by Pix2pixHD [23], for local detail refinement and global structure adjustment.

In this stage, we use the multi-scale discriminators D_{fs} and the coarse-to-fine generator G_{fs} following Pix2pixHD [23]. Specifically, the generator G_{fs} consists of two sub-networks $G1$ and $G2$, both of which follow encoder-decoder architecture, as shown on the right part of Fig. 7. We sample the output of the first stage using a downsampling operation with a sampling rate of 50%. This newly sampled image $X_{intact}^{1/2}$ ($height/2, width/2$) is then fed into the first sub-network $G1$, which is designed to capture global features. The other sub-network $G2$ is employed to capture the local details, which takes the output of the first stage as input. We use both concatenation and element-wise addition operations to fuse the style, local, and global information. Specifically, the concatenation combines the style feature map and the output of $G1$ and generates a new fused feature map. Then, the element-wise addition is utilized to combine this new feature map with the latent feature of the encoder part of $G2$. Finally, we use the decoder part of $G2$ to generate the final output X_o . It is worth noting that the style vector can control the style of the generated sketches, which helps improve their quality and diversity. Besides, the style of the real photo is often fixed, and independent from the artists' style. Therefore,

we introduce the style information in the I2S task but exclude that in the S2I task.

4.4 Loss Function

We use a combination of several loss functions to train our model. We denote X and Y as the input and its corresponding reference, respectively. For simplicity, we define $G(X)$ as the generated output of the given input X and $D_k(X, Y)$ as the corresponding predicted probabilities of the k -th discriminator. Then, we denote the i -th layer feature extractor of discriminator D_k as D_k^i , where k is the index of the discriminator.

Adversarial Loss. We use the adversarial loss [73] to make the generated image more visually appealing. The adversarial loss we use is defined as:

$$L_{adv}(G, D) = \mathbb{E}_{X, Y}[\log D(X, Y)] + \mathbb{E}_X[1 - \log D(X, G(X))]. \quad (1)$$

Feature Matching Loss. Similar to [23], we use the feature matching loss to improve the adversarial loss based on the k -th discriminator. The feature matching loss is defined as:

$$L_{fm}(G, D_k) = \mathbb{E}_{X, Y} \sum_{i=0}^T \frac{1}{N_i} [\|D_k^i(X, Y) - D_k^i(X, G(X))\|_1], \quad (2)$$

where T denotes the total number of layers in each discriminator and N_i is the number of feature maps in the i -th layer. This loss is used to match the intermediate feature maps of the real and synthesized image, making the generator produce multi-scale statistical information. Besides, it stabilizes the training process and restores highly realistic outputs.

Perceptual Loss. To maintain perceptual and semantic consistency, we use a perceptual loss [93] to measure the difference between the original image and the corresponding synthesized image. We extract the perceptual features from the i -th layer activations of a pre-trained VGGNet [89], which is denoted as $\phi_i(\cdot)$. The perceptual loss is defined as follows:

$$L_{per}(G(X), Y) = \mathbb{E}_{G(X), Y} \sum_{i=0}^t \|\phi_i(Y) - \phi_i(G(X))\|_1. \quad (3)$$

Pixel-Wise Loss. The L_1 distance between a generated image $G(X)$ and reference Y is regarded as the pixel-wise loss, which is defined as:

$$L_1(G(X), Y) = \frac{1}{h \times w} \sum_{(i,j)=(0,0)}^{(h,w)} \|Y(i,j) - G(X)_{(i,j)}\|_1, \quad (4)$$

where (i,j) and (h,w) are the pixel coordinates and the (height, width) of the output, respectively.

Style Classification Loss. Similar to [181, 182], we define an auxiliary classifier to predict the sketch style of the generated image. For any generated image $G(X)$, the style classification loss is defined as:

$$L_{\text{sty}}(G, S, c) = \mathbb{E}_{X,c} [l_{\text{ce}}(S(G(X)), c)], \quad (5)$$

where $l_{\text{ce}}(\cdot, \cdot)$ is the cross-entropy loss, $S(\cdot)$ is a CNN that outputs the probability over different styles, and c is the label of a given artist's style. Note that we only use the style classification loss in the second stage for the I2S task.

Overall Loss. Finally, the overall loss function for the multi-scale discriminators is:

$$L_{D \sim (D_{\text{parts}}, D_{\text{fs}})} = \sum_i^K -L_{\text{adv}} + \lambda_{\text{fm}} L_{\text{fm}}, \quad (6)$$

and the overall loss function for generator is:

$$L_{G \sim (G_{\text{parts}}, G_{\text{fs}})} = L_{\text{adv}} + \lambda_{\text{fm}} L_{\text{fm}} + \lambda_1 L_1 + \lambda_{\text{per}} L_{\text{per}} + \lambda_{\text{sty}} L_{\text{sty}}, \quad (7)$$

where λ_{fm} , λ_1 , λ_{per} , and λ_{sty} are hyperparameters that control the importance of the feature matching loss, pixel-wise loss, perceptual loss, and style classification loss, respectively.

4.5 Implementation Details

We use PyTorch [183] to implement the baseline FSGAN. The experiments are conducted on an NVIDIA V100S.

For the I2S task, we set $\lambda_{\text{fm}} = 25.0$, $\lambda_1 = 25.0$, and $\lambda_{\text{per}} = 12.5$ to train the model in the facial components synthesis stage, and set $\lambda_{\text{fm}} = 100.0$, $\lambda_1 = 100.0$, $\lambda_{\text{per}} = 50.0$, and $\lambda_{\text{sty}} = 100.0$ for facial synthesis. The Adam optimizer [184] is used for training the whole network. The initial learning rates for the generator and discriminator are $2e-4$

and $1e-5$, respectively. The other hyperparameters of the optimizer are set to the default values as recommended in PyTorch. We set the number of epochs to 50. All generators and discriminators are trained iteratively.

For the S2I task, we set $\lambda_{\text{fm}} = 50.0$, $\lambda_1 = 50.0$, and $\lambda_{\text{per}} = 0.2$ to train the neural network for facial components synthesis stage, and set $\lambda_{\text{fm}} = 100.0$, $\lambda_1 = 100.0$, and $\lambda_{\text{per}} = 0.2$ for facial synthesis. We again use the Adam optimizer, with initial learning rates of $2e-4$ for both the generators and discriminators. The training strategy is almost the same as that for the I2S task. However, we set the number of epochs to 400,¹⁴ freezing the weights of the facial components synthesis module after 250 epochs and further training the facial synthesis module for the remaining epochs.

5 Benchmark

This section provides comprehensive comparisons and analyses of the existing models on FS2K, in terms of both the I2S and S2I tasks.

5.1 Experimental Settings

5.1.1 Evaluation Metrics

For the I2S task, the most popular facial sketch metric is the structural similarity index metric (SSIM) [20, 44]. However, it ignores the perceptual similarity between a prediction and the reference. Therefore, we further adopt the recently proposed structure co-occurrence texture (SCOOT) metric [29], which provides a unified evaluation for both structure and texture. For the S2I task, we still adopt the widely used SSIM metric to evaluate the synthesized faces. Our evaluation toolbox is available at <https://github.com/DengPingFan/FS2KToolbox>.

5.1.2 Compared Models

To evaluate the performance on the I2S task and S2I task, we present the empirical results of 19 representative approaches and FSGAN baseline.

¹⁴Because the S2I task needs to restore more detailed information of the RGB images, more training epochs are required.

Table 5 Quantitative results of popular models on the I2S task. “↑” means the higher, the better. Publ.: Publication information.

#	Model	Publ.	SCOOT↑	SSIM↑
1	DualGAN [78]	Yi <i>et al.</i> ICCV	0.261	0.324
2	FPST [95]	Chen <i>et al.</i> NeurIPS	0.271	0.460
3	NST [87, 88]	Gatys <i>et al.</i> CVPR	0.273	0.326
4	Pix2pix [31]	Isola <i>et al.</i> CVPR	0.275	0.438
5	ACL-GAN [79]	Zhao <i>et al.</i> ECCV	0.278	0.404
6	WCT [99]	Li <i>et al.</i> NeurIPS	0.282	0.369
7	AdaIN [98]	Huang <i>et al.</i> ICCV	0.303	0.365
8	UNIT [22]	Liu <i>et al.</i> NeurIPS	0.304	0.504
9	TSIT [80]	Jiang <i>et al.</i> ECCV	0.307	0.441
10	DRIT++ [27]	Lee <i>et al.</i> IJCV	0.308	0.492
11	CartoonGAN [85]	Chen <i>et al.</i> CVPR	0.319	0.400
12	UGATIT [30]	Kim <i>et al.</i> ICLR	0.323	0.457
13	NICE-GAN [26]	Chen <i>et al.</i> CVPR	0.327	0.473
14	CycleGAN [21]	Zhu <i>et al.</i> ICCV	0.348	0.435
15	MDAL [11]	Zhang <i>et al.</i> TNNLS	0.355	0.466
16	UPDG [9]	Yi <i>et al.</i> CVPR	0.364	0.471
17	Pix2pixHD [23]	Wang <i>et al.</i> CVPR	0.374	0.492
18	APDrawing [2]	Yi <i>et al.</i> CVPR	0.375	0.464
19	DSMAP [25]	Chang <i>et al.</i> ECCV	0.378	0.493
20	FSGAN	Fan <i>et al.</i> MIR	0.405	0.510

5.1.3 Training/Testing Protocols

All compared methods are selected based on three criteria: a) widely regarded technology, b) open-source code, and c) state-of-the-art performance. The models are trained and tested on our FS2K with the image sizes specified in their papers. If the size setting is not provided in their paper, 512×512 is utilized as default.

5.2 Overall Results and Analysis

5.2.1 I2S Task

We first provide a performance summary of the I2S task regarding both SCOOT and SSIM scores. Quantitative results and qualitative comparisons are shown in Table 5 and Fig. 8-10, respectively. The experimental observations indicate that FSGAN baseline achieves better results. For further analysis, we divide all compared methods into three categories based on their SCOOT score:

- score ≤ 0.3 ;
- $0.3 < \text{score} \leq 0.35$;
- $0.35 < \text{score}$.

Analysis. Methods in the first group achieve a SCOOT below 0.3. These include DualGAN [78], FPST [95], NST [87, 88], Pix2pix [31], ACL-GAN [79], and WCT [99]. As shown in Fig. 8, DualGAN, NST, and WCT suffer from structural distortion, where many local facial details are lost. The images produced by the DualGAN are poor, and it is challenging to detect facial components

in them. This explains why it has lower SSIM and SCOOT scores. In addition, compared with other results, Pix2pix and FPST generate blur results. ACL-GAN seems to achieve satisfactory results in visual appeal, yielding a higher SSIM score. However, ACL-GAN reproduces the original facial structure almost exactly, lacking artistic style.

The second group includes AdaIN [98], UNIT [22], TSIT [80], DRIT++ [27], CartoonGAN [85], UGATIT [30], NICE-GAN [26], and CycleGAN [21], whose SCOOT scores range from 0.3 to 0.35. As shown in Fig. 9, the synthesized sketch images are better in terms of structure-preserving compared to the first group. However, except for AdaIN, all models are thrown off by the complex backgrounds (see the hair region in the second row). Besides, the results of CartoonGAN seem to alter the color of the input images, leading to lower SSIM scores.

MDAL [11], UPDG [9], Pix2pixHD [23], APDrawing [2], DSMAP [25], and FSGAN baseline are categorized into the third group, which can generate sketches without distortion or losing too much of the global details. However, UPDG and APDrawing miss some details in the hair region, leading to poor visual effects. APDrawing introduces a lot of extra strokes, especially for the first sketch style. Besides, APDrawing usually results in a lack and distortion of the local structure, as seen in the hair region. Meanwhile, the sketches generated by UPDG have better style elements, but the model cannot handle complex backgrounds. Pix2pixHD generates

Table 6 Quantitative results of popular models on the S2I task. “↑” means the higher, the better.

#	Model	Publication	SSIM↑
1	DualGAN [78]	Yi <i>et al.</i> ICCV	0.241
2	WCT [99]	Li <i>et al.</i> NeurIPS	0.311
3	ACL-GAN [79]	Zhao <i>et al.</i> ECCV	0.314
4	TSIT [80]	Jiang <i>et al.</i> ECCV	0.316
5	UGATIT [30]	Kim <i>et al.</i> ICLR	0.317
6	NST [87, 88]	Gatys <i>et al.</i> CVPR	0.335
7	CycleGAN [21]	Zhu <i>et al.</i> ICCV	0.339
8	Pix2pix [31]	Isola <i>et al.</i> CVPR	0.346
9	SPADE [24]	Park <i>et al.</i> CVPR	0.361
10	UNIT [22]	Liu <i>et al.</i> NeurIPS	0.362
11	AdaIN [98]	Huang <i>et al.</i> ICCV	0.373
12	DRIT++ [27]	Lee <i>et al.</i> IJCV	0.381
13	FNS [93]	Johnson <i>et al.</i> ECCV	0.391
14	NICE-GAN [26]	Chen <i>et al.</i> CVPR	0.397
15	FPST [95]	Chen <i>et al.</i> NeurIPS	0.400
16	pSp [86]	Richardson <i>et al.</i> CVPR	0.428
17	Pix2pixHD [23]	Wang <i>et al.</i> CVPR	0.433
18	DSMAP [25]	Chang <i>et al.</i> ECCV	0.471
19	DeepPS [149]	Yang <i>et al.</i> ECCV	0.487
20	FSGAN	Fan <i>et al.</i> MIR	0.503

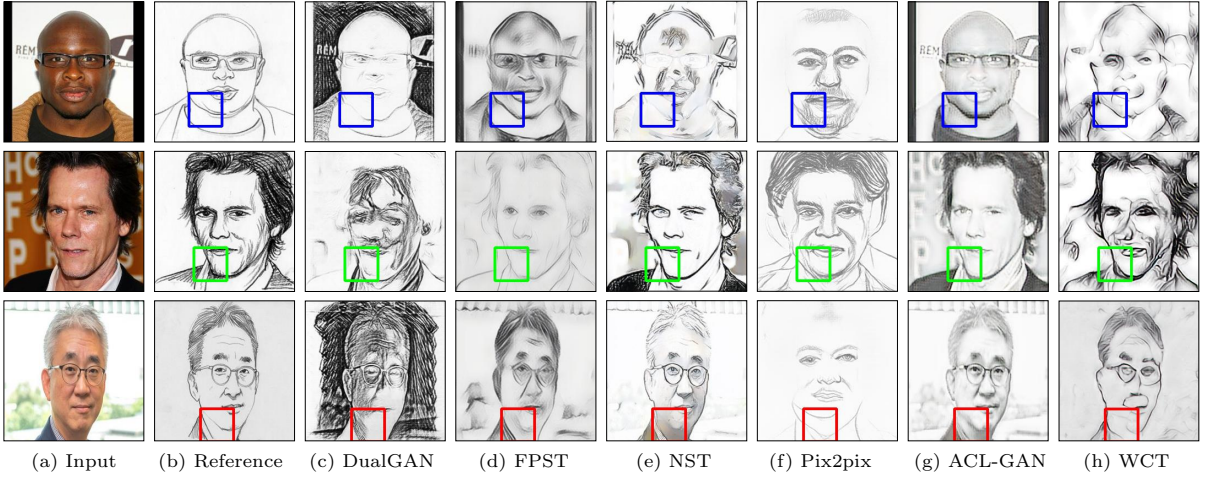


Fig. 8 From left to right: input face, reference, DualGAN [78], FPST [95], NST [87, 88], Pix2pix [31], ACL-GAN [79], and WCT [99]. We mark the three styles with blue, green, and red boxes for each result. Zoom-in for details.

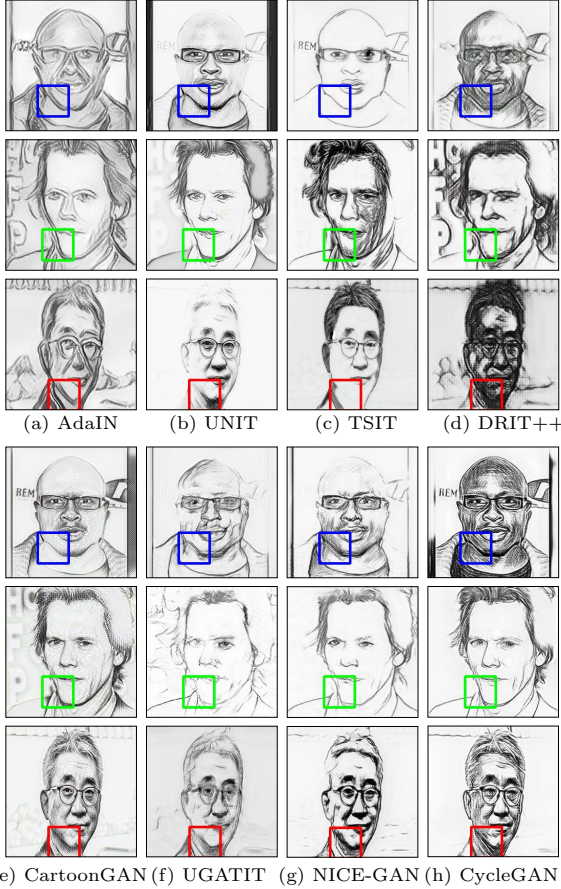


Fig. 9 Comparison of AdaIN [98], UNIT [22], TSIT [80], DRIT++ [27], CartoonGAN [85], UGATIT [30], NICE-GAN [26], and CycleGAN [21]. Their inputs and references are shown in Fig. 8.

relatively good sketches with global structure and clean background, but it does not generate the best facial components. For example, in Fig. 10-e, the region around the eyes is unclear, and many details are lost. Take the third row, for instance; the eyeglasses are partially lost, while the eyeball is entirely black. We further observe that DMAP and MDAL tend to achieve better sketch images but with distortions in local facial information. Finally, the baseline can synthesize high-quality sketches that focus on the global structure and local details while considering diverse styles. Moreover, as shown in the highlighted boxes (with green, blue and red), we find that the outputs of FSGAN are more similar to the reference compared to other state-of-the-arts.

5.2.2 S2I Task

We report our experimental results in Table 6 and Fig. 11. We find that FSGAN achieves the best results on our challenging FS2K compared to the existing state-of-the-art models.

Analysis. As seen in Fig. 11, we observe that most compared methods are unable to successfully recover accurate images, revealing that the S2I task is more complicated than I2S. We argue that this is because the sketches are highly abstract, and the loss of valuable information makes it difficult for neural networks to restore the original image. We also observe that the high-resolution models, such as Pix2pixHD and FSGAN, tend to output more visually appealing results.

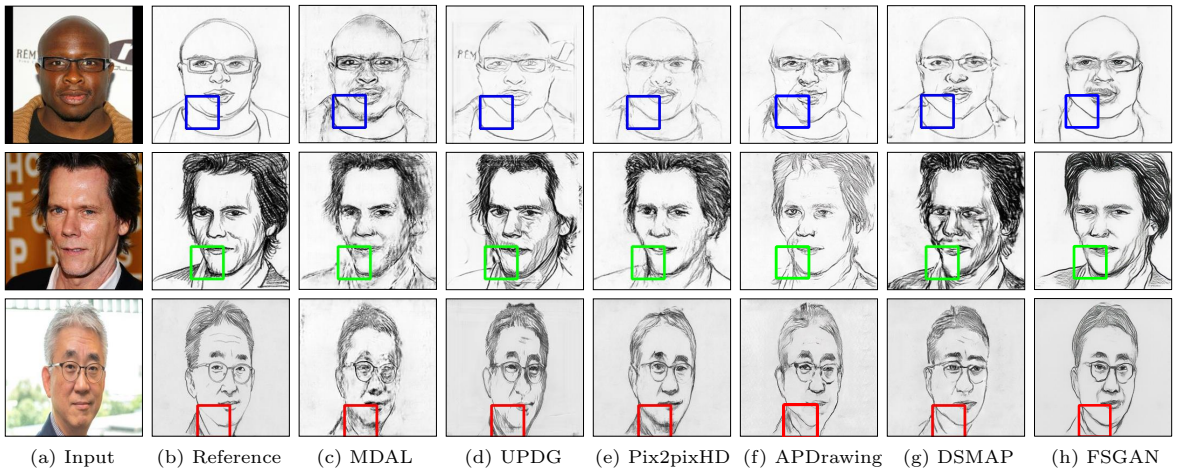


Fig. 10 Comparison results with MDAL [11], UPDG [9], Pix2pixHD [23], APDrawing [2], and DSMAP [25].

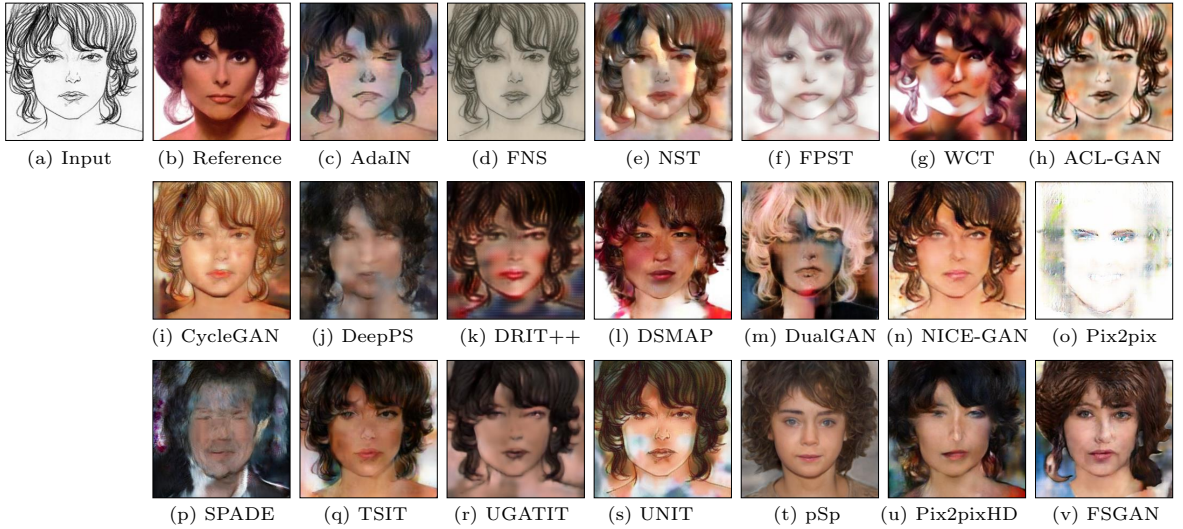


Fig. 11 We select 19 classical models, including AdaIN [98], FNS [93], FPST [95], WCT [99], ACL-GAN [79], CycleGAN [21], DeepPS [149], DRIT++ [27], DSMAP [25], DualGAN [78], NICE-GAN [26], Pix2pix [31], SPADE [24], TSIT [80], UGATIT [30], UNIT [22], pSp [86], and Pix2pixHD [23], for qualitative comparison.

The results presented in Fig. 11 show that FNS and FPST fail to transfer the sketches into colored images. SPADE and Pix2pix generate poor results with facial outlines (*e.g.*, Pix2pix) or black backgrounds (*e.g.*, SPADE). Five models (*i.e.*, NST, WCT, DeepPS, DSMAP, and UNIT) produce noise patches in salient regions, which corrupt the global facial structure. Meanwhile, AdaIN, ACL-GAN, DualGAN, and UGATIT perform better than the models mentioned above, resulting in unrealistic cartoon-style images. Only CycleGAN, NICE-GAN, TSIT, pSp, and Pix2pixHD overcome various challenges and achieve good

results in terms of facial completeness. In particular, the eye regions from Pix2pixHD [23] and pSp [86] are better than other models. However, compared with the results of FSGAN, the facial features of Pix2pixHD are relatively inferior because a pixel-wise rather than block-wise strategy learns. Although pSp [86] can generate high-quality results, its results lack diversity compared with FSGAN baseline. For example, pSp generates similar facial expressions under two different sketch styles, while baseline can synthesize diverse contents, as shown in Fig. 12.

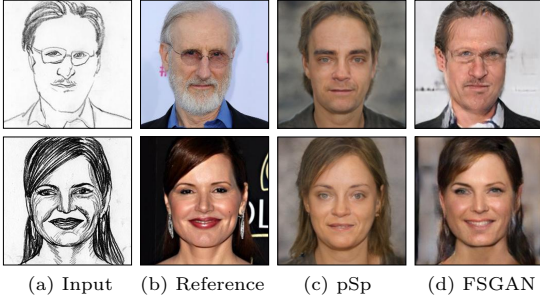


Fig. 12 Visual diversity of the data generated for S2I task.

5.3 Attribute-Based Analysis

5.3.1 SCOOT Metric Results

To provide a deeper understanding of the models, we present an attribute-based performance evaluation in Table 7.

Analysis. Hair is one of the dominant features of the head. In Table 7, we find that most models achieve slightly better or comparable performance on images without hair than with, except for three models, such as AdaIN, CartoonGAN, and CycleGAN. Meanwhile, we find that red and black hair are the most challenging and easiest to detect/reconstruct, respectively. We argue that this is because images with red and black hair make up the lowest and largest (>40%) proportion of all data, respectively. Thus, the models are unfamiliar/familiar with these attributes.

In addition, we also notice that females (F) are more challenging than males (M) for almost all models since women usually have various accessories and hairstyles. For example, the models perform worse on images with earrings (w/ E) than those without earrings. Also, the facial images with smiles are more challenging than those without smiles. Interestingly, existing models achieve diverse performance irrespective of the color of hair (*e.g.*, H(b), H(bl), H(r), and H(g)). Finally, compared to style 1 (simple lines) and style 3 (*i.e.*, repeated wispy details), we see that style 2 (long strokes) is the most challenging for all models.

5.3.2 SSIM Metric Results

In addition to the SCOOT metric, we also provide the SSIM metric for the I2S task in Table 8.

Analysis. We find that the overall performance tends to be similar to the SCOOT metric results in several key attributes, such as hair, gender, accessories, and style. We notice that the

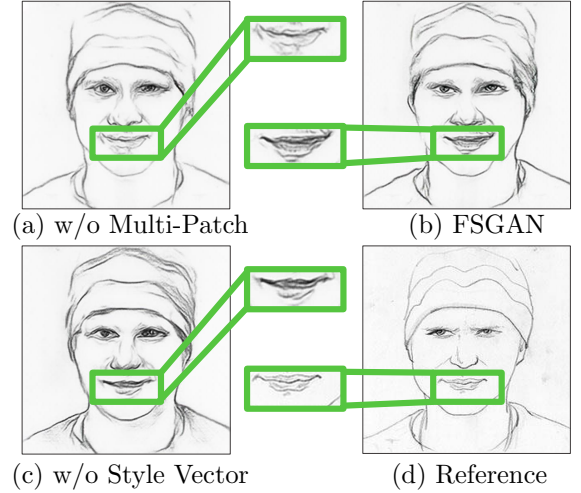


Fig. 13 Ablation study for the I2S task.

performance on “w/ F” is lower than on “w/o F”, as shown in Table 8. One possible reason is that frontal faces preserve more structural features than non-frontal ones. Therefore, in the I2S task, images with attributes such as “w/ F” are more challenging than “w/o F”.

5.4 Ablation Study

This section provides a detailed analysis of FSGAN on the proposed FS2K dataset. Unlike most existing facial synthesis models [23], our model has a two-stage GAN architecture for both I2S and S2I tasks. Besides, a sketch style vector is introduced to enable diversified style synthesis in the second stage of the I2S task. Therefore, the ablation studies on the I2S task are conducted on the following two key components: (1) the facial components synthesis stage and (2) the style vector assisted generation. Note that we adopt the same hyperparameters described in Sec. 4.5 during our ablation experiments.

Table 9 shows the ablation results for the I2S task. We find that the facial components synthesis stage increases the SCOOT and SSIM scores by 1.31% (relative) and 2.67%, respectively, while the style vector increases them by 6.30% and 4.72%. As illustrated in Fig. 13, without the multi-patch strategy, the lines in the synthesized lips are often missing structure details. Meanwhile, with the multi-patch stage, the lines become smoother. Moreover, the synthesized drawings are

Table 7 Comparison of 19 state-of-the-art models in terms of attribute-based performance on the I2S task. Here, w/ H = hair visible, w/o H = hair invisible, H(b) = brown hair, H(bl) = black hair, H(r) = red hair, H(g) = golden hair, M = male, F = female, w/ E = with earring, w/o E = without earring, w/ S = with smile, w/o S = without smile, w/ F = frontal face, w/o F = non-frontal face, S1 = style1, S2 = style2, and S3 = style3.

Model		SCOOT↑																
		w/ H	w/o H	H(b)	H(bl)	H(r)	H(g)	M	F	w/ E	w/o E	w/ S	w/o S	w/ F	w/o F	S1	S2	S3
CartoonGAN	DualGAN [78]	0.260	0.279	0.250	0.267	0.216	0.279	0.275	0.240	0.239	0.266	0.255	0.271	0.261	0.262	0.298	0.194	0.319
	FPST [95]	0.269	0.304	0.254	0.294	0.214	0.304	0.288	0.245	0.246	0.276	0.262	0.286	0.269	0.278	0.329	0.168	0.332
	NST [87, 88]	0.272	0.283	0.268	0.287	0.236	0.283	0.280	0.262	0.258	0.276	0.268	0.282	0.272	0.276	0.310	0.205	0.332
	Pix2pix [31]	0.272	0.335	0.255	0.300	0.217	0.335	0.298	0.240	0.250	0.281	0.267	0.290	0.276	0.272	0.333	0.178	0.302
	ACL-GAN [79]	0.276	0.309	0.265	0.298	0.226	0.309	0.292	0.256	0.254	0.283	0.270	0.291	0.276	0.284	0.330	0.183	0.355
	WCT [99]	0.281	0.315	0.271	0.302	0.229	0.315	0.296	0.261	0.262	0.287	0.277	0.292	0.281	0.290	0.332	0.195	0.346
	AdaIN [98]	0.303	0.295	0.307	0.317	0.258	0.295	0.306	0.298	0.283	0.307	0.298	0.310	0.300	0.314	0.348	0.215	0.419
	UNIT [22]	0.301	0.364	0.292	0.328	0.225	0.364	0.330	0.265	0.261	0.313	0.293	0.324	0.301	0.319	0.376	0.175	0.411
	TSIT [80]	0.307	0.307	0.308	0.320	0.259	0.307	0.320	0.288	0.283	0.313	0.300	0.320	0.306	0.316	0.359	0.208	0.432
	DRIT++ [27]	0.305	0.348	0.291	0.336	0.248	0.348	0.329	0.276	0.279	0.314	0.299	0.323	0.305	0.323	0.380	0.181	0.378
	CartoonGAN [85]	0.319	0.318	0.320	0.337	0.262	0.318	0.329	0.304	0.291	0.325	0.314	0.329	0.317	0.332	0.382	0.204	0.428
	UGATIT [30]	0.321	0.365	0.315	0.347	0.265	0.365	0.339	0.298	0.298	0.328	0.314	0.338	0.322	0.325	0.391	0.204	0.400
	NICE-GAN [26]	0.325	0.355	0.320	0.357	0.262	0.355	0.342	0.303	0.302	0.332	0.317	0.343	0.325	0.333	0.398	0.201	0.401
	CycleGAN [21]	0.348	0.343	0.358	0.362	0.287	0.343	0.351	0.343	0.326	0.353	0.341	0.360	0.346	0.357	0.397	0.252	0.483
	MDAL [11]	0.354	0.363	0.348	0.380	0.292	0.363	0.369	0.333	0.329	0.360	0.345	0.372	0.352	0.365	0.436	0.211	0.446
UPDG [9]	0.362	0.411	0.349	0.390	0.290	0.411	0.390	0.325	0.336	0.371	0.356	0.379	0.363	0.370	0.423	0.259	0.448	
APDrawing [2]	0.374	0.395	0.372	0.399	0.322	0.395	0.380	0.369	0.356	0.380	0.370	0.385	0.373	0.390	0.456	0.227	0.524	
Pix2pixHD [23]	0.374	0.392	0.365	0.403	0.307	0.385	0.392	0.351	0.343	0.378	0.371	0.392	0.371	0.381	0.462	0.212	0.508	
DSMAP [25]	0.375	0.431	0.357	0.405	0.322	0.431	0.400	0.343	0.354	0.383	0.369	0.393	0.377	0.381	0.437	0.276	0.423	
FSGAN		0.403	0.435	0.389	0.435	0.335	0.435	0.423	0.377	0.381	0.410	0.395	0.422	0.403	0.414	0.481	0.268	0.509

Table 8 Comparison of 19 top models in terms of attribute-based performance on the I2S task.

Model	SSIM↑																	
	w/ H	w/o H	H(b)	H(bl)	H(r)	H(g)	M	F	w/ E	w/o E	w/ S	w/o S	w/ F	w/o F	S1	S2	S3	
DualGAN [78]	0.320	0.393	0.310	0.342	0.276	0.393	0.352	0.282	0.292	0.331	0.313	0.343	0.318	0.354	0.364	0.247	0.424	
FPST [95]	0.459	0.481	0.442	0.492	0.383	0.481	0.492	0.411	0.416	0.469	0.448	0.481	0.455	0.486	0.517	0.351	0.597	
NST [87, 88]	0.325	0.347	0.317	0.349	0.256	0.347	0.339	0.306	0.305	0.330	0.316	0.344	0.324	0.338	0.372	0.241	0.417	
Pix2pix [31]	0.434	0.526	0.410	0.470	0.332	0.526	0.478	0.377	0.391	0.449	0.425	0.461	0.438	0.439	0.503	0.319	0.558	
ACL-GAN [79]	0.402	0.432	0.392	0.430	0.334	0.432	0.427	0.369	0.363	0.413	0.393	0.423	0.398	0.434	0.445	0.316	0.583	
WCT [99]	0.368	0.389	0.368	0.387	0.316	0.389	0.389	0.339	0.334	0.377	0.362	0.381	0.367	0.380	0.407	0.297	0.461	
AdaIN [98]	0.364	0.367	0.364	0.382	0.319	0.367	0.378	0.343	0.340	0.370	0.359	0.375	0.362	0.379	0.399	0.297	0.460	
UNIT [22]	0.501	0.556	0.488	0.528	0.421	0.556	0.539	0.450	0.460	0.514	0.492	0.526	0.498	0.532	0.563	0.395	0.616	
TSIT [80]	0.439	0.465	0.430	0.461	0.371	0.465	0.465	0.404	0.408	0.448	0.431	0.458	0.435	0.468	0.485	0.351	0.587	
DRIT++ [27]	0.490	0.534	0.479	0.519	0.411	0.534	0.524	0.444	0.451	0.501	0.480	0.512	0.487	0.515	0.547	0.387	0.617	
CartoonGAN [85]	0.399	0.420	0.397	0.421	0.345	0.420	0.419	0.372	0.368	0.407	0.392	0.416	0.395	0.425	0.438	0.321	0.552	
UGATIT [30]	0.455	0.497	0.445	0.476	0.386	0.497	0.489	0.409	0.416	0.466	0.447	0.476	0.451	0.491	0.499	0.373	0.593	
NICE-GAN [26]	0.472	0.497	0.463	0.492	0.398	0.497	0.505	0.424	0.429	0.483	0.464	0.490	0.468	0.498	0.518	0.384	0.603	
CycleGAN [21]	0.433	0.461	0.429	0.455	0.374	0.461	0.460	0.395	0.401	0.442	0.425	0.452	0.429	0.463	0.471	0.358	0.580	
MDAL [11]	0.465	0.487	0.457	0.491	0.399	0.487	0.496	0.420	0.426	0.475	0.458	0.481	0.462	0.488	0.506	0.386	0.593	
UPDG [9]	0.468	0.507	0.456	0.500	0.391	0.507	0.501	0.424	0.431	0.479	0.459	0.493	0.465	0.501	0.534	0.355	0.584	
APDrawing [2]	0.461	0.522	0.441	0.497	0.373	0.522	0.504	0.402	0.419	0.473	0.452	0.484	0.458	0.492	0.512	0.371	0.582	
Pix2pixHD [23]	0.492	0.552	0.473	0.523	0.419	0.546	0.531	0.431	0.457	0.505	0.481	0.513	0.488	0.524	0.537	0.402	0.618	
DSMAP [25]	0.490	0.551	0.472	0.527	0.405	0.551	0.532	0.433	0.447	0.503	0.481	0.515	0.488	0.518	0.557	0.373	0.622	
FSGAN	0.507	0.565	0.491	0.539	0.424	0.565	0.549	0.451	0.466	0.520	0.498	0.531	0.505	0.534	0.568	0.403	0.629	

messier without the style vector component and may introduce shadows in the lip regions.

For the S2I task, an ablation study is conducted to validate the effectiveness of the facial components synthesis stage, as shown in Table 10. Like the I2S task, the multi-patch component achieves a significant performance gain (*i.e.*, 3.3%) over the baseline model. Fig. 14 provides examples of the results produced by our model and the model without the facial components synthesis

stage. As we can see, our model with facial components synthesis captures more details and ensures a more realistic overall appearance (see Fig. 14-c).

6 Discussion

Although FSS has achieved significant progress, there is still a large room for improvement. This section summarizes the possible future research directions related to FSS.



(a) Input (b) w/o multi-patch (c) FSGAN

Fig. 14 Ablation study for the S2I task.**Table 9** Ablation study of FSGAN on the I2S task.

Setting	multi-patch	style vec.	SCOOT \uparrow	SSIM \uparrow
Baseline			0.381	0.487
	✓		0.386 (+1.31%)	0.500 (+2.67%)
FSGAN	✓	✓	0.405 (+6.30%)	0.510 (+4.72%)

Table 10 Ablation study of our model on the S2I task.

Setting	multi-patch	SSIM \uparrow
Baseline		0.487
FSGAN	✓	0.503 (+3.3%)

(1) Datasets. Due to the relative shortage of professional sketch artists, achieving large numbers of images remains an open problem, impeding the development of FSS. Furthermore, more diversified sketch (or drawing) styles are needed to build more attractive models and achieve better synthesis results. To address these issues, we believe novel data augmentation techniques [116, 185, 186] and transfer learning strategies [187–189] designed for FSS are promising directions of study.

(2) Models. Currently, most state-of-the-art models are trained with a large number of paired images, and sketches [9, 23] to overcome data shortages. However, more attention could be paid to techniques like few-shot [190], semi-supervised [191], weakly-supervised [192], self-supervised [193], and non-pairwise unsupervised [83] learning to achieve the style transfer with limited datasets. Besides, developing novel, human-in-the-loop [194] models is another promising direction, which would provide more interactive options to users for generating and editing personalized styles. Interactive models that utilize the attributes in our FS2K could also serve as drawing tools provided to professional artists for facilitating the creation of sketches and other styles of drawing. Furthermore, FSS in the wild is still challenging because the image quality, including resolution, noise, and background, varies drastically. In addition to the techniques mentioned above, basic model units could also be focused

on to develop new strategies. For example, most current models are built upon CNN [195] units. Therefore, more exploration of other frameworks, such as MLPs [196] and Transformers [197, 198], could also be conducted.

(3) Evaluation. Evaluation metrics are essential for the development of new models and the benchmarking of existing ones. Currently, several quantitative evaluation metrics [20, 199] and human visual ranking methods [66] are used. However, as these aim to provide relatively objective and fair comparisons between all models, the different applications of FSS are not considered. This may lead to biased or unreliable evaluation of specific tasks. Therefore, more task-specific evaluation metrics and methods could be another important direction for future research.

(4) Applications. Currently, the only direct applications of FSS (I2S and S2I) are entertainment, and law enforcement [1, 44]. With the development of FSS techniques, many other promising applications could also be implicitly or explicitly facilitated by FSS research, such as art design, animation production, *etc.* In addition to these industrial applications, we believe that FSS methods and ideas could also benefit other research fields. For example, sketches could be used to assist image resizing [200], super-resolution [201], *etc.* Further, the sketches usually contain the most conspicuous information of an image and can therefore be considered compressed versions of RGB images [202]. This characteristic makes sketches useful for the image compression task. Besides, the S2I task can be considered a specific case of image super-resolution in a broad sense because both tasks aim to reconstruct detailed RGB images from the given inputs. The difference is that the input of S2I is high-frequency information, while that of the standard super-resolution task is the low-frequency information of the original image.

7 Conclusion

We have presented a complete review of the facial-sketch synthesis problem. To the best of our knowledge, this is the first systematic study on deep FSS in sketch-to-image and image-to-sketch tasks. To achieve this, we established a new challenging dataset, named FS2K. We also introduced a copy table for the proposed FS2K to

address the alignment issue between the sketches drawn by artists and the original images. The proposed simple baseline, FSGAN, achieves the new state-of-the-art performance with a two-stage architecture. Finally, as the most extensive survey (*i.e.*, 89 literature methods) and benchmark (*i.e.*, 19 cutting-edge models), we have revealed that the development of this field is still in its infancy. Therefore, the main goal of this paper is to spark novel ideas rather than rank all benchmarked works. It isn't easy to benchmark all of the existing models due to the prosperity of the field. We hope this investigation will attract the community's attention and yield exciting follow-up directions, such as generating vivid sketches with music, developing cartoons from sketches, synthesizing sketch videos, and fake face [203], *etc.*

References

- [1] X. Wang and X. Tang, "Face photo-sketch synthesis and recognition," *IEEE TPAMI*, 2009.
- [2] R. Yi, Y.-J. Liu, Y.-K. Lai, and P. L. Rosin, "APDrawingGAN: Generating artistic portrait drawings from face photos with hierarchical GANs," in *CVPR*, 2019.
- [3] H. Koshimizu, M. Tominaga, T. Fujiwara, and K. Murakami, "On kansei facial image processing for computerized facial caricaturing system picasso," in *CSMC*, 1999.
- [4] H. S. Bhatt, S. Bharadwaj, R. Singh, and M. Vatsa, "On matching sketches with digital face images," in *BTAS*, 2010.
- [5] W. Zhang, X. Wang, and X. Tang, "Coupled information-theoretic encoding for face photo-sketch recognition," in *CVPR*, 2011.
- [6] N. Wang, X. Gao, D. Tao, and X. Li, "Face sketch-photo synthesis under multi-dictionary sparse representation framework," in *ICIG*, 2011.
- [7] X. Gao, N. Wang, D. Tao, and X. Li, "Face sketch-photo synthesis and retrieval using sparse representation," *IEEE TCSVT*, 2012.
- [8] I. Berger, A. Shamir, M. Mahler, E. Carter, and J. Hodgins, "Style and abstraction in portrait sketching," *ACM TOG*, 2013.
- [9] R. Yi, Y.-J. Liu, Y.-K. Lai, and P. L. Rosin, "Unpaired portrait drawing generation via asymmetric cycle mapping," in *CVPR*, 2020.
- [10] R. Yi, M. Xia, Y.-J. Liu, Y.-K. Lai, and P. L. Rosin, "Line drawings for face portraits from photos using global and local structure based GANs," *IEEE TPAMI*, 2020.
- [11] S. Zhang, R. Ji, J. Hu, X. Lu, and X. Li, "Face sketch synthesis by multidomain adversarial learning," *IEEE TNNLS*, 2018.
- [12] M. Zhu, J. Li, N. Wang, and X. Gao, "Knowledge distillation for face photo-sketch synthesis," *IEEE TNNLS*, 2020.
- [13] N. Kumar, A. C. Berg, P. N. Belhumeur, and S. K. Nayar, "Attribute and simile classifiers for face verification," in *ICCV*, 2009.
- [14] H.-S. Du, Q.-P. Hu, D.-F. Qiao, and I. Pitas, "Robust face recognition via low-rank sparse representation-based classification," *IJAC*, 2015.
- [15] Y.-Z. Lu, "A novel face recognition algorithm for distinguishing faces with various angles," *IJAC*, 2008.
- [16] V. Jain and E. Learned-Miller, "Fddb: A benchmark for face detection in unconstrained settings," UMass Amherst technical report, Tech. Rep., 2010.
- [17] Z. Zhang, P. Luo, C. C. Loy, and X. Tang, "Facial landmark detection by deep multi-task learning," in *ECCV*, 2014.
- [18] A. Bulat and G. Tzimiropoulos, "How far are we from solving the 2d & 3d face alignment problem?(and a dataset of 230,000 3d facial landmarks)," in *ICCV*, 2017.

- [19] J. Sun, Q. Li, W. Wang, J. Zhao, and Z. Sun, “Multi-caption text-to-face synthesis: Dataset and algorithm,” in *ACM MM*, 2021.
- [20] Z. Wang, A. C. Bovik, H. R. Sheikh, and E. P. Simoncelli, “Image quality assessment: from error visibility to structural similarity,” *IEEE TIP*, 2004.
- [21] J.-Y. Zhu, T. Park, P. Isola, and A. A. Efros, “Unpaired image-to-image translation using cycle-consistent adversarial networks,” in *ICCV*, 2017.
- [22] M.-Y. Liu, T. Breuel, and J. Kautz, “Unsupervised image-to-image translation networks,” in *NeurIPS*, 2017.
- [23] T.-C. Wang, M.-Y. Liu, J.-Y. Zhu, A. Tao, J. Kautz, and B. Catanzaro, “High-resolution image synthesis and semantic manipulation with conditional GANs,” in *CVPR*, 2018.
- [24] T. Park, M.-Y. Liu, T.-C. Wang, and J.-Y. Zhu, “Semantic image synthesis with spatially-adaptive normalization,” in *CVPR*, 2019.
- [25] H.-Y. Chang, Z. Wang, and Y.-Y. Chuang, “Domain-specific mappings for generative adversarial style transfer,” in *ECCV*, 2020.
- [26] R. Chen, W. Huang, B. Huang, F. Sun, and B. Fang, “Reusing discriminators for encoding: Towards unsupervised image-to-image translation,” in *CVPR*, 2020.
- [27] H.-Y. Lee, H.-Y. Tseng, Q. Mao, J.-B. Huang, Y.-D. Lu, M. K. Singh, and M.-H. Yang, “DRIT++: Diverse image-to-image translation via disentangled representations,” *IJCV*, 2020.
- [28] Z. Liu, P. Luo, X. Wang, and X. Tang, “Deep learning face attributes in the wild,” in *ICCV*, 2015.
- [29] D.-P. Fan, S. Zhang, Y.-H. Wu, Y. Liu, M.-M. Cheng, B. Ren, P. L. Rosin, and R. Ji, “Scoot: A perceptual metric for facial sketches,” in *ICCV*, 2019.
- [30] J. Kim, M. Kim, H. Kang, and K. Lee, “Ugat-it: unsupervised generative attentional networks with adaptive layer-instance normalization for image-to-image translation,” in *ICLR*, 2020.
- [31] P. Isola, J.-Y. Zhu, T. Zhou, and A. A. Efros, “Image-to-image translation with conditional adversarial networks,” in *CVPR*, 2017.
- [32] C. Peng, X. Gao, N. Wang, and J. Li, “Face recognition from multiple stylistic sketches: Scenarios, datasets, and evaluation,” *PR*, 2018.
- [33] A. M. Martinez, “The ar face database,” *CVC Technical Report24*, 1998.
- [34] K. Messer, J. Matas, J. Kittler, J. Luetin, G. Maitre *et al.*, “XM2VTSDB: The extended m2vts database,” in *ICABPA*, 1999.
- [35] P. J. Phillips, H. Moon, S. A. Rizvi, and P. J. Rauss, “The FERET evaluation methodology for face-recognition algorithms,” *IEEE TPAMI*, 2000.
- [36] Á. Serrano, I. M. de Diego, C. Conde, E. Cabello, L. Shen, and L. Bai, “Influence of wavelet frequency and orientation in an SVM-based parallel gabor PCA face verification system,” in *ICIDEAL*, 2007.
- [37] H. S. Bhatt, S. Bharadwaj, R. Singh, and M. Vatsa, “Memetically optimized MCWLD for matching sketches with digital face images,” *IEEE TIFS*, 2012.
- [38] M. Minear and D. C. Park, “A lifespan database of adult facial stimuli,” *Behav. Res. Meth. Instrum. Comput.*, 2004.
- [39] J. Nishino, T. Kamyama, H. Shira, T. Odaka, and H. Ogura, “Linguistic knowledge acquisition system on facial caricature drawing system,” in *ICFS*, 1999.

- [40] S. Iwashita, Y. Takeda, and T. Onisawa, "Expressive facial caricature drawing," in *ICFS*, 1999.
- [41] Y. Li and H. Kobatake, "Extraction of facial sketch image based on morphological processing," in *ICIP*, 1997.
- [42] M. Tominaga, S. Fukuoka, K. Murakami, and H. Koshimizu, "Facial caricaturing with motion caricaturing in PICASSO system," in *ICAIM*, 1997.
- [43] S. E. Brennan, "Caricature generator," Ph.D. dissertation, MIT, 1982.
- [44] N. Wang, D. Tao, X. Gao, X. Li, and J. Li, "A Comprehensive Survey to Face Hallucination," *IJCV*, 2013.
- [45] H. Chen, Y.-Q. Xu, H.-Y. Shum, S.-C. Zhu, and N.-N. Zheng, "Example-based facial sketch generation with non-parametric sampling," in *ICCV*, 2001.
- [46] A. V. Nefian and M. H. Hayes III, "Face recognition using an embedded hmm," in *AVBPA*, 1999.
- [47] X. Gao, J. Zhong, J. Li, and C. Tian, "Face sketch synthesis algorithm based on e-hmm and selective ensemble," *IEEE TCSVT*, 2008.
- [48] Z. Xu, H. Chen, S.-C. Zhu, and J. Luo, "A hierarchical compositional model for face representation and sketching," *IEEE TPAMI*, 2008.
- [49] W. Zhang, X. Wang, and X. Tang, "Lighting and pose robust face sketch synthesis," in *ECCV*, 2010.
- [50] H. Zhou, Z. Kuang, and K.-Y. K. Wong, "Markov weight fields for face sketch synthesis," in *CVPR*, 2012.
- [51] T. Wang, J. P. Collomosse, A. Hunter, and D. Greig, "Learnable stroke models for example-based portrait painting," in *BMVC*, 2013.
- [52] N. Wang, D. Tao, X. Gao, X. Li, and J. Li, "Transductive face sketch-photo synthesis," *IEEE TNNLS*, 2013.
- [53] C. Peng, X. Gao, N. Wang, and J. Li, "Superpixel-based face sketch-photo synthesis," *IEEE TCSVT*, 2015.
- [54] C. Peng, X. Gao, N. Wang, D. Tao, X. Li, and J. Li, "Multiple representations-based face sketch-photo synthesis," *IEEE TNNLS*, 2015.
- [55] H. Abdi and L. J. Williams, "Principal component analysis," *Wiley interdisciplinary reviews: computational statistics*, 2010.
- [56] X. Tang and X. Wang, "Face photo recognition using sketch," in *ICIP*, 2002.
- [57] X. Tang and X. Wang, "Face sketch synthesis and recognition," in *ICCV*, 2003.
- [58] X. Tang and X. Wang, "Face sketch recognition," *IEEE TCSVT*, 2004.
- [59] Q. Liu, X. Tang, H. Jin, H. Lu, and S. Ma, "A nonlinear approach for face sketch synthesis and recognition," in *CVPR*, 2005.
- [60] D.-A. Huang and Y.-C. F. Wang, "Coupled dictionary and feature space learning with applications to cross-domain image synthesis and recognition," in *ICCV*, 2013.
- [61] N. Ji, X. Chai, S. Shan, and X. Chen, "Local regression model for automatic face sketch generation," in *ICIG*, 2011.
- [62] L. Chang, M. Zhou, X. Deng, Z. Wu, and Y. Han, "Face sketch synthesis via multi-variate output regression," in *HCI*, 2011.
- [63] J. Zhang, N. Wang, X. Gao, D. Tao, and X. Li, "Face sketch-photo synthesis based on support vector regression," in *ICIP*, 2011.
- [64] S. T. Roweis and L. K. Saul, "Nonlinear dimensionality reduction by locally linear embedding," *Science*, 2000.
- [65] S. Wang, L. Zhang, Y. Liang, and Q. Pan, "Semi-coupled dictionary learning with

- applications to image super-resolution and photo-sketch synthesis,” in *CVPR*, 2012.
- [66] Y. Song, L. Bao, Q. Yang, and M.-H. Yang, “Real-time exemplar-based face sketch synthesis,” in *ECCV*, 2014.
- [67] N. Wang, X. Gao, and J. Li, “Random sampling for fast face sketch synthesis,” *PR*, 2018.
- [68] S. Zhang, X. Gao, N. Wang, and J. Li, “Robust face sketch style synthesis,” *IEEE TIP*, 2015.
- [69] Y. Li, Y.-Z. Song, T. M. Hospedales, and S. Gong, “Free-hand sketch synthesis with deformable stroke models,” *IJCV*, 2017.
- [70] J. Li, X. Yu, C. Peng, and N. Wang, “Adaptive representation-based face sketch-photo synthesis,” *Neurocomputing*, 2017.
- [71] Y. Men, Z. Lian, Y. Tang, and J. Xiao, “A common framework for interactive texture transfer,” in *CVPR*, 2018.
- [72] S. Saxena and M. N. Teli, “Comparison and analysis of image-to-image generative adversarial networks: A survey,” 2021.
- [73] I. J. Goodfellow, J. Pouget-Abadie, M. Mirza, B. Xu, D. Warde-Farley, S. Ozair, A. Courville, and Y. Bengio, “Generative adversarial networks,” in *NeurIPS*, 2014.
- [74] M. Mirza and S. Osindero, “Conditional generative adversarial nets,” in *NeurIPS*, 2014.
- [75] O. Ronneberger, P. Fischer, and T. Brox, “U-net: Convolutional networks for biomedical image segmentation,” in *MICCAI*, 2015.
- [76] J.-Y. Zhu, R. Zhang, D. Pathak, T. Darrell, A. A. Efros, O. Wang, and E. Shechtman, “Toward multimodal image-to-image translation,” in *NeurIPS*, 2017.
- [77] T. Kim, M. Cha, H. Kim, J. K. Lee, and J. Kim, “Learning to discover cross-domain relations with generative adversarial networks,” in *ICML*, 2017.
- [78] Z. Yi, H. Zhang, P. Tan, and M. Gong, “DualGAN: Unsupervised dual learning for image-to-image translation,” in *ICCV*, 2017.
- [79] Y. Zhao, R. Wu, and H. Dong, “Unpaired image-to-image translation using adversarial consistency loss,” in *ECCV*, 2020.
- [80] L. Jiang, C. Zhang, M. Huang, C. Liu, J. Shi, and C. C. Loy, “TSIT: A simple and versatile framework for image-to-image translation,” in *ECCV*, 2020.
- [81] P. Zhang, B. Zhang, D. Chen, L. Yuan, and F. Wen, “Cross-domain correspondence learning for exemplar-based image translation,” in *CVPR*, 2020.
- [82] X. Zhou, B. Zhang, T. Zhang, P. Zhang, J. Bao, D. Chen, Z. Zhang, and F. Wen, “CoCosNet v2: Full-resolution correspondence learning for image translation,” in *CVPR*, 2021.
- [83] A. Chen, R. Liu, L. Xie, Z. Chen, H. Su, and J. Yu, “Sofgan: A portrait image generator with dynamic styling,” *ACM TOG*, 2022.
- [84] Y. Jing, Y. Yang, Z. Feng, J. Ye, Y. Yu, and M. Song, “Neural style transfer: A review,” *IEEE TVCG*, 2019.
- [85] Y. Chen, Y.-K. Lai, and Y.-J. Liu, “Cartoongan: Generative adversarial networks for photo cartoonization,” in *CVPR*, 2018.
- [86] E. Richardson, Y. Alaluf, O. Patashnik, Y. Nitzan, Y. Azar, S. Shapiro, and D. Cohen-Or, “Encoding in style: a stylegan encoder for image-to-image translation,” in *CVPR*, 2021.
- [87] L. A. Gatys, A. S. Ecker, and M. Bethge, “A neural algorithm of artistic style,” *arXiv preprint arXiv:1508.06576*, 2015.
- [88] L. A. Gatys, A. S. Ecker, and M. Bethge, “Image style transfer using convolutional neural networks,” in *CVPR*, 2016.
- [89] K. Simonyan and A. Zisserman, “Very deep convolutional networks for large-scale image

- recognition,” in *ICLR*, 2015.
- [90] T. Karras, S. Laine, and T. Aila, “A style-based generator architecture for generative adversarial networks,” in *CVPR*, 2019.
 - [91] R. Abdal, Y. Qin, and P. Wonka, “Image2styleGAN: How to embed images into the stylegan latent space?” in *ICCV*, 2019.
 - [92] D. Kotovenko, M. Wright, A. Heimbrecht, and B. Ommer, “Rethinking style transfer: From pixels to parameterized brushstrokes,” *CVPR*, 2021.
 - [93] J. Johnson, A. Alahi, and L. Fei-Fei, “Perceptual losses for real-time style transfer and super-resolution,” in *ECCV*, 2016.
 - [94] D. Ulyanov, V. Lebedev, A. Vedaldi, and V. S. Lempitsky, “Texture networks: Feed-forward synthesis of textures and stylized images,” in *ICML*, 2016.
 - [95] T. Q. Chen and M. Schmidt, “Fast patch-based style transfer of arbitrary style,” in *NeurIPS*, 2016.
 - [96] V. Dumoulin, J. Shlens, and M. Kudlur, “A learned representation for artistic style,” *ICLR*, 2017.
 - [97] D. Ulyanov, A. Vedaldi, and V. Lempitsky, “Improved texture networks: Maximizing quality and diversity in feed-forward stylization and texture synthesis,” in *CVPR*, 2017.
 - [98] X. Huang and S. Belongie, “Arbitrary style transfer in real-time with adaptive instance normalization,” in *ICCV*, 2017.
 - [99] Y. Li, C. Fang, J. Yang, Z. Wang, X. Lu, and M.-H. Yang, “Universal style transfer via feature transforms,” in *NeurIPS*, 2017.
 - [100] M. Eitz, J. Hays, and M. Alexa, “How do humans sketch objects?” *ACM TOG*, 2012.
 - [101] P. J. Phillips, H. Wechsler, J. Huang, and P. J. Rauss, “The feret database and evaluation procedure for face-recognition algorithms,” *IMAVIS*, 1998.
 - [102] T.-Y. Lin, M. Maire, S. Belongie, J. Hays, P. Perona, D. Ramanan, P. Dollár, and C. L. Zitnick, “Microsoft coco: Common objects in context,” in *ECCV*, 2014.
 - [103] O. Russakovsky, J. Deng, H. Su, J. Krause, S. Satheesh, S. Ma, Z. Huang, A. Karpathy, A. Khosla, M. Bernstein, A. C. Berg, and L. Fei-Fei, “ImageNet large scale visual recognition challenge,” *IJCV*, 2015.
 - [104] M. Cimpoi, S. Maji, I. Kokkinos, S. Mohamed, and A. Vedaldi, “Describing textures in the wild,” in *CVPR*, 2014.
 - [105] S. Y. Duck, “Painter by numbers, wikiart.org,” in <https://www.kaggle.com/c/painter-by-numbers>, 2016.
 - [106] M. Cordts, M. Omran, S. Ramos, T. Rehfeld, M. Enzweiler, R. Benenson, U. Franke, S. Roth, and B. Schiele, “The cityscapes dataset for semantic urban scene understanding,” in *CVPR*, 2016.
 - [107] R. Tyleček and R. Šára, “Spatial pattern templates for recognition of objects with regular structure,” in *GCPR*, 2013.
 - [108] J.-Y. Zhu, P. Krähenbühl, E. Shechtman, and A. A. Efros, “Generative visual manipulation on the natural image manifold,” in *ECCV*, 2016.
 - [109] A. Yu and K. Grauman, “Fine-grained visual comparisons with local learning,” in *CVPR*, 2014.
 - [110] P.-Y. Laffont, Z. Ren, X. Tao, C. Qian, and J. Hays, “Transient attributes for high-level understanding and editing of outdoor scenes,” *ACM TOG*, 2014.
 - [111] Y. LeCun, L. Bottou, Y. Bengio, and P. Haffner, “Gradient-based learning applied to document recognition,” *IEEE*,

- 1998.
- [112] C. Wah, S. Branson, P. Welinder, P. Perona, and S. Belongie, “The caltech-ucsd birds-200-2011 dataset,” 2011.
 - [113] T. Karras, T. Aila, S. Laine, and J. Lehtinen, “Progressive growing of GANs for improved quality, stability, and variation,” in *ICLR*, 2018.
 - [114] N. Silberman, D. Hoiem, P. Kohli, and R. Fergus, “Indoor segmentation and support inference from rgb-d images,” in *ECCV*, 2012.
 - [115] B. Zhou, H. Zhao, X. Puig, S. Fidler, A. Barriuso, and A. Torralba, “Scene parsing through ade20k dataset,” in *CVPR*, 2017.
 - [116] Q. Yu, Y.-Z. Song, T. Xiang, and T. M. Hospedales, “Sketchx!-shoe/chair fine-grained SBIR dataset,” 2017.
 - [117] D. Ha and D. Eck, “A neural representation of sketch drawings,” in *ICLR*, 2018.
 - [118] Y. Jin, J. Zhang, M. Li, Y. Tian, H. Zhu, and Z. Fang, “Towards the automatic anime characters creation with generative adversarial networks,” in *NeurIPS*, 2017.
 - [119] H. Xu, Y. Gao, F. Yu, and T. Darrell, “End-to-end learning of driving models from large-scale video datasets,” in *CVPR*, 2017.
 - [120] G. Ros, L. Sellart, J. Materzynska, D. Vazquez, and A. M. Lopez, “The synthia dataset: A large collection of synthetic images for semantic segmentation of urban scenes,” in *CVPR*, 2016.
 - [121] Z. Liu, P. Luo, S. Qiu, X. Wang, and X. Tang, “Deepfashion: Powering robust clothes recognition and retrieval with rich annotations,” in *CVPR*, 2016.
 - [122] E. Agustsson and R. Timofte, “Ntire 2017 challenge on single image super-resolution: Dataset and study,” in *CVPRW*, 2017.
 - [123] B. Yao, X. Yang, and S.-C. Zhu, “Introduction to a large-scale general purpose ground truth database: methodology, annotation tool and benchmarks,” in *CVPRW*, 2007.
 - [124] J. Krause, M. Stark, J. Deng, and L. Fei-Fei, “3d object representations for fine-grained categorization,” in *ICCVW*, 2013.
 - [125] F. Yu, A. Seff, Y. Zhang, S. Song, T. Funkhouser, and J. Xiao, “Lsun: Construction of a large-scale image dataset using deep learning with humans in the loop,” *arXiv preprint arXiv:1506.03365*, 2015.
 - [126] X. Huang, M.-Y. Liu, S. Belongie, and J. Kautz, “Multimodal unsupervised image-to-image translation,” in *ECCV*, 2018.
 - [127] L. Zhang, L. Lin, X. Wu, S. Ding, and L. Zhang, “End-to-end photo-sketch generation via fully convolutional representation learning,” in *ICMR*, 2015.
 - [128] M. Zhu, N. Wang, X. Gao, and J. Li, “Deep graphical feature learning for face sketch synthesis,” in *IJCAI*, 2017.
 - [129] P. Sangkloy, J. Lu, C. Fang, F. Yu, and J. Hays, “Scribbler: Controlling deep image synthesis with sketch and color,” in *CVPR*, 2017.
 - [130] M. Zhang, N. Wang, Y. Li, R. Wang, and X. Gao, “Face sketch synthesis from coarse to fine,” in *AAAI*, 2018.
 - [131] W. Xian, P. Sangkloy, V. Agrawal, A. Raj, J. Lu, C. Fang, F. Yu, and J. Hays, “TextureGAN: Controlling deep image synthesis with texture patches,” in *CVPR*, 2018.
 - [132] J. Song, K. Pang, Y.-Z. Song, T. Xiang, and T. M. Hospedales, “Learning to sketch with shortcut cycle consistency,” in *CVPR*, 2018.
 - [133] Y. Lu, S. Wu, Y.-W. Tai, and C.-K. Tang, “Image generation from sketch constraint using contextual GAN,” in *ECCV*, 2018.

- [134] S. Zhang, R. Ji, J. Hu, Y. Gao, and C.-W. Lin, “Robust face sketch synthesis via generative adversarial fusion of priors and parametric sigmoid,” in *IJCAI*, 2018.
- [135] M. Zhang, N. Wang, X. Gao, and Y. Li, “Markov random neural fields for face sketch synthesis,” in *IJCAI*, 2018.
- [136] L. Wang, V. Sindagi, and V. Patel, “High-quality facial photo-sketch synthesis using multi-adversarial networks,” in *ICAFGR*, 2018.
- [137] M. Zhang, R. Wang, X. Gao, J. Li, and D. Tao, “Dual-transfer face sketch-photo synthesis,” *IEEE TIP*, 2018.
- [138] H. Kazemi, M. Iranmanesh, A. Dabouei, S. Soleymani, and N. M. Nasrabadi, “Facial attributes guided deep sketch-to-photo synthesis,” in *WACVW*, 2018.
- [139] H. Kazemi, F. Taherkhani, and N. M. Nasrabadi, “Unsupervised facial geometry learning for sketch to photo synthesis,” in *BIOSIG*, 2018.
- [140] S. You, N. You, and M. Pan, “Pi-rec: Progressive image reconstruction network with edge and color domain,” *arXiv preprint arXiv:1903.10146*, 2019.
- [141] M. Zhang, N. Wang, Y. Li, and X. Gao, “Deep latent low-rank representation for face sketch synthesis,” *IEEE TNNLS*, 2019.
- [142] M. Zhu, J. Li, N. Wang, and X. Gao, “A deep collaborative framework for face photo-sketch synthesis,” *IEEE TNNLS*, 2019.
- [143] M. Zhang, Y. Li, N. Wang, Y. Chi, and X. Gao, “Cascaded face sketch synthesis under various illuminations,” *IEEE TIP*, 2019.
- [144] M. Zhu, N. Wang, X. Gao, J. Li, and Z. Li, “Face photo-sketch synthesis via knowledge transfer,” in *IJCAI*, 2019.
- [145] Y. Li, C. Fang, A. Hertzmann, E. Shechtman, and M.-H. Yang, “Im2pencil: Controllable pencil illustration from photographs,” in *CVPR*, 2019.
- [146] A. Ghosh, R. Zhang, P. K. Dokania, O. Wang, A. A. Efros, P. H. Torr, and E. Shechtman, “Interactive sketch & fill: Multiclass sketch-to-image translation,” in *ICCV*, 2019.
- [147] X. Wang and J. Yu, “Learning to cartoonize using white-box cartoon representations,” in *CVPR*, 2020.
- [148] C. Gao, Q. Liu, Q. Xu, L. Wang, J. Liu, and C. Zou, “Sketchycoco: image generation from freehand scene sketches,” in *CVPR*, 2020.
- [149] S. Yang, Z. Wang, J. Liu, and Z. Guo, “Deep plastic surgery: Robust and controllable image editing with human-drawn sketches,” in *ECCV*, 2020.
- [150] S.-Y. Chen, W. Su, L. Gao, S. Xia, and H. Fu, “DeepFaceDrawing: Deep generation of face images from sketches,” *ACM TOG*, 2020.
- [151] J. Yu, X. Xu, F. Gao, S. Shi, M. Wang, D. Tao, and Q. Huang, “Toward realistic face photo-sketch synthesis via composition-aided gans,” *IEEE TCYB*, 2020.
- [152] Y. Fang, W. Deng, J. Du, and J. Hu, “Identity-aware CycleGAN for face photo-sketch synthesis and recognition,” *PR*, 2020.
- [153] Y. Lin, S. Ling, K. Fu, and P. Cheng, “An identity-preserved model for face sketch-photo synthesis,” *IEEE SPL*, 2020.
- [154] C. Peng, N. Wang, J. Li, and X. Gao, “Universal face photo-sketch style transfer via multiview domain translation,” *IEEE TIP*, 2020.
- [155] S. Duan, Z. Chen, Q. J. Wu, L. Cai, and D. Lu, “Multi-scale gradients self-attention residual learning for face photo-sketch transformation,” *IEEE TIFS*, 2020.

- [156] S.-Y. Wang, D. Bau, and J.-Y. Zhu, “Sketch your own GAN,” in *ICCV*, 2021.
- [157] A. K. Bhunia, S. Khan, H. Cholakal, R. M. Anwer, F. S. Khan, J. Laaksonen, and M. Felsberg, “Doodleformer: Creative sketch drawing with transformers,” *arXiv preprint arXiv:2112.03258*, 2021.
- [158] Y. Song, C. Yang, Y. Shen, P. Wang, Q. Huang, and C.-C. J. Kuo, “Spg-net: Segmentation prediction and guidance network for image inpainting,” in *BMVC*, 2018.
- [159] D. Yi, Z. Lei, S. Liao, and S. Z. Li, “Learning face representation from scratch,” *arXiv preprint arXiv:1411.7923*, 2014.
- [160] L. Wang, R.-F. Li, K. Wang, and J. Chen, “Feature representation for facial expression recognition based on facs and lbp,” *IJAC*, 2014.
- [161] X. Zheng, Y. Guo, H. Huang, Y. Li, and R. He, “A survey of deep facial attribute analysis,” *IJCV*, 2020.
- [162] G. B. Huang, M. Mattar, T. Berg, and E. Learned-Miller, “Labeled faces in the wild: A database for studying face recognition in unconstrained environments,” in *FRLIW*, 2008.
- [163] R. Ranjan, V. M. Patel, and R. Chellappa, “Hyperface: A deep multi-task learning framework for face detection, landmark localization, pose estimation, and gender recognition,” *IEEE TPAMI*, 2017.
- [164] E. M. Hand and R. Chellappa, “Attributes for improved attributes: A multi-task network utilizing implicit and explicit relationships for facial attribute classification,” in *AAAI*, 2017.
- [165] H. Han, A. K. Jain, F. Wang, S. Shan, and X. Chen, “Heterogeneous face attribute estimation: A deep multi-task learning approach,” *IEEE TPAMI*, 2017.
- [166] Y. Jang, H. Gunes, and I. Patras, “Smilenet: registration-free smiling face detection in the wild,” in *ICCVW*, 2017.
- [167] R. Ranjan, S. Sankaranarayanan, C. D. Castillo, and R. Chellappa, “An all-in-one convolutional neural network for face analysis,” in *FG*, 2017.
- [168] S. Li and W. Deng, “Deep facial expression recognition: A survey,” *IEEE TAC*, 2020.
- [169] N. Zhang, M. Paluri, M. Ranzato, T. Darrell, and L. Bourdev, “Panda: Pose aligned networks for deep attribute modeling,” in *CVPR*, 2014.
- [170] M. Kan, S. Shan, H. Chang, and X. Chen, “Stacked progressive auto-encoders (spae) for face recognition across poses,” in *CVPR*, 2014.
- [171] Y. Wu, Z. Wang, and Q. Ji, “Facial feature tracking under varying facial expressions and face poses based on restricted boltzmann machines,” in *CVPR*, 2013.
- [172] L. Tran, X. Yin, and X. Liu, “Disentangled representation learning GAN for pose-invariant face recognition,” in *CVPR*, 2017.
- [173] U. Toseeb, D. R. Keeble, and E. J. Bryant, “The significance of hair for face recognition,” *PloS one*, 2012.
- [174] S. J. Bartel, K. Toews, L. Gronhøvd, and S. L. Prime, “Do i know you? altering hairstyle affects facial recognition,” *VC*, 2018.
- [175] N. Kumar, P. Belhumeur, and S. Nayar, “Facetracer: A search engine for large collections of images with faces,” in *ECCV*, 2008.
- [176] L. Huai-Yu, D. Wei-Ming, and B.-G. Hu, “Facial image attributes transformation via conditional recycle generative adversarial networks,” *JCST*, 2018.
- [177] J.-S. Pierrard and T. Vetter, “Skin detail analysis for face recognition,” in *CVPR*, 2007.

- [178] S. Z. Li, *Encyclopedia of Biometrics: I-Z*. Springer Science & Business Media, 2009.
- [179] K. Zhang, Z. Zhang, Z. Li, and Y. Qiao, “Joint face detection and alignment using multitask cascaded convolutional networks,” *IEEE SPL*, 2016.
- [180] K. He, X. Zhang, S. Ren, and J. Sun, “Deep residual learning for image recognition,” in *CVPR*, 2016.
- [181] Y. Choi, M. Choi, M. Kim, J.-W. Ha, S. Kim, and J. Choo, “StarGAN: Unified generative adversarial networks for multi-domain image-to-image translation,” in *CVPR*, 2018.
- [182] B. Zhao, B. Chang, Z. Jie, and L. Sigal, “Modular generative adversarial networks,” in *ECCV*, 2018.
- [183] A. Paszke, S. Gross, S. Chintala, G. Chanan, E. Yang, Z. DeVito, Z. Lin, A. Desmaison, L. Antiga, and A. Lerer, “Automatic differentiation in pytorch,” in *NeurIPSW*, 2017.
- [184] D. P. Kingma and J. Ba, “Adam: A method for stochastic optimization,” in *ICLR*, 2014.
- [185] Q. Yu, F. Liu, Y.-Z. Song, T. Xiang, T. M. Hospedales, and C.-C. Loy, “Sketch me that shoe,” in *CVPR*, 2016.
- [186] C. Shorten and T. M. Khoshgoftaar, “A survey on image data augmentation for deep learning,” *JBD*, 2019.
- [187] Y. Wang, C. Wu, L. Herranz, J. van de Weijer, A. Gonzalez-Garcia, and B. Raducanu, “Transferring gans: generating images from limited data,” in *ECCV*, 2018.
- [188] L. Yu, J. van de Weijer *et al.*, “Deepi2i: Enabling deep hierarchical image-to-image translation by transferring from gans,” in *NeurIPS*, 2020.
- [189] A. Shocher, Y. Gandelsman, I. Mosseri, M. Yarom, M. Irani, W. T. Freeman, and T. Dekel, “Semantic pyramid for image generation,” in *ICCV*, 2020.
- [190] S. Ravi and H. Larochelle, “Optimization as a model for few-shot learning,” in *ICLR*, 2017.
- [191] O. Chapelle, B. Scholkopf, and A. Zien, Eds., “Semi-supervised learning (chapelle, o. et al., eds.; 2006) [book reviews],” *IEEE TNN*, 2009.
- [192] M. Oquab, L. Bottou, I. Laptev, and J. Sivic, “Is object localization for free? - weakly-supervised learning with convolutional neural networks,” in *CVPR*, 2015.
- [193] X. Wang, K. He, and A. Gupta, “Transitive invariance for self-supervised visual representation learning,” in *ICCV*, 2017.
- [194] R. Pinto, T. Mettler, and M. Taisch, “Managing supplier delivery reliability risk under limited information: Foundations for a human-in-the-loop DSS,” *DSS*, 2013.
- [195] Y. LeCun *et al.*, “Generalization and network design strategies,” *CIP*, 1989.
- [196] I. O. Tolstikhin, N. Houlsby, A. Kolesnikov, L. Beyer, X. Zhai, T. Unterthiner, J. Yung, A. Steiner, D. Keysers, J. Uszkoreit *et al.*, “Mlp-mixer: An all-mlp architecture for vision,” in *NeurIPS*, 2021.
- [197] A. Vaswani, N. Shazeer, N. Parmar, J. Uszkoreit, L. Jones, A. N. Gomez, L. Kaiser, and I. Polosukhin, “Attention is all you need,” in *NeurIPS*, 2017.
- [198] K. Lee, H. Chang, L. Jiang, H. Zhang, Z. Tu, and C. Liu, “ViTGAN: Training GANs with vision transformers,” in *ICLR*, 2022.
- [199] L. Zhang, L. Zhang, X. Mou, and D. Zhang, “Fsim: A feature similarity index for image quality assessment,” *IEEE TIP*, 2011.
- [200] S. Avidan and A. Shamir, “Seam carving for content-aware image resizing,” *ACM TOG*, 2007.

- [201] C. Dong, C. C. Loy, K. He, and X. Tang, “Image super-resolution using deep convolutional networks,” *IEEE TPAMI*, 2015.
- [202] Y. Hu, S. Yang, W. Yang, L.-Y. Duan, and J. Liu, “Towards coding for human and machine vision: A scalable image coding approach,” in *ICME*, 2020.
- [203] E. Wood, T. Baltrušaitis, C. Hewitt, S. Dziadzio, T. J. Cashman, and J. Shotton, “Fake it till you make it: Face analysis in the wild using synthetic data alone,” in *ICCV*, 2021.

Deng-Ping Fan received his PhD degree from the Nankai University in 2019. He joined Inception Institute of Artificial Intelligence (IIAI) in 2019. He has published about 50 top journal and conference papers such as TPAMI, CVPR, ICCV, ECCV, etc. His research interests include computer vision, deep learning, and visual attention, especially the human vision on co-salient object detection, RGB salient object detection, RGB-D salient object detection, and video salient object detection. He won the Best Paper Finalist Award at IEEE CVPR 2019, the Best Paper Award Nominee at IEEE CVPR 2020. He was recognized as the CVPR 2019 outstanding reviewer with a special mention award, the CVPR 2020 outstanding reviewer, the ECCV 2020 high-quality reviewer, and the CVPR 2021 outstanding reviewer. He served as a program committee board (PCB) member of IJCAI 2022-2024, a senior program committee (SPC) member of IJCAI 2021, a committee member of China Society of Image and Graphics (CSIG), area chair in NeurIPS 2021 Datasets and Benchmarks Track, area chair in MICCAI2020 Wshp (OMIA7), editorial board member of the Computer Vision & AI.

E-mail: dengpfan@gmail.com

ORCID iD: 0000-0002-5245-7518

Ziling Huang received the B.S. degree in electrical engineering from North China Electric Power University, Beijing, China, in 2015, and the master degree in Electrical Engineering from National Tsing Hua University, Hsinchu, Taiwan in 2020. She has been pursuing her Ph.D. degree at the Department of Information and Communication

Engineering, Graduate School of Information Science and Technology, the University of Tokyo since September 2020. She was an intern student at National Institute of Informatics, Tokyo, Japan, in 2019, and at ByteDance, Beijing, China, from 2019 to 2020. Her research interests include computer vision and machine learning.

E-mail: huangziling@nii.ac.jp

ORCID iD: 0000-0003-3241-7911

Peng Zheng is pursuing his master degree in Visual Computing and Communication programme from Aalto University and University of Trento. He was a research intern at Inception Institute of Artificial Intelligence (IIAI) from March 2021 to October 2021. He has been a research assistant in MBZUAI since January 2022. He serves as the reviewer of IEEE TPAMI. His research interests include computer vision and machine learning, especially on common information mining and person search.

E-mail: zhengpeng0108@gmail.com

ORCID iD: 0000-0002-4087-5237

Hong Liu obtained his Ph.D. degree from Xiamen University, China, in 2020. He is now a JSPS Fellowship researcher at the National Institute of Informatics, Japan. His research interests include large-scale image retrieval, Riemannian-based machine learning, and deep adversarial learning. He has published about 20+ papers in top journals and conferences such as TPAMI, IJCV, TIP, CVPR, ICCV, ECCV, ICLR, etc. He was awarded the Outstanding Doctoral Dissertation Award of the China Society of Image and Graphics, JSPS International Fellowship, and Top-100 Chinese New Stars in Artificial Intelligence by Baidu Scholar.

E-mail: hliu@nii.ac.jp

ORCID iD: 0000-0001-5318-6388

Xuebin Qin obtained his PhD degree from the University of Alberta, Edmonton, Canada, in 2020. Since March, 2020, He is a Postdoctoral Fellow in the Department of Computing Science and the Department of Radiology and Diagnostic Imaging, University of Alberta, Canada. His research interests include highly accurate image segmentation, salient object detection, image

labeling and detection. He has published about 10 papers in vision and robotics conferences such as CVPR, BMVC, ICPR, WACV, IROS, *etc.*

E-mail: xuebin@ualberta.ca

ORCID iD: 0000-0001-9875-983X

Luc Van Gool received the degree in electromechanical engineering at the Katholieke Universiteit Leuven in 1981. Currently, he is a professor at the Katholieke Universiteit Leuven in Belgium and the ETH in Zurich, Switzerland. He leads computer vision research at both places, and also teaches at both. He has been a program committee member of several major computer vision conferences. His main interests include 3D reconstruction and modeling, object recognition, tracking, and gesture analysis, and the combination of those. He received several Best Paper awards, won a David Marr Prize and a Koenderink Award, and was nominated Distinguished Researcher by the IEEE Computer Science committee. He is a co-founder of 10 spin-off companies.

E-mail: vangool@vision.ee.ethz.ch